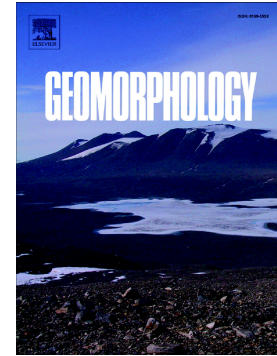


Journal Pre-proof

Integrating historical, geomorphological and sedimentological insights to reconstruct past floods: Insights from Kea Point, Mt. Cook Village, Aotearoa New Zealand

R.D. Williams, H.M. Griffiths, J.R. Carr, A.J. Hepburn, M. Gibson, J.J. Williams, T.D.L. Irvine-Fynn



PII: S0169-555X(21)00436-0

DOI: <https://doi.org/10.1016/j.geomorph.2021.108028>

Reference: GEOMOR 108028

To appear in: *Geomorphology*

Received date: 16 December 2020

Revised date: 1 November 2021

Accepted date: 3 November 2021

Please cite this article as: R.D. Williams, H.M. Griffiths, J.R. Carr, et al., Integrating historical, geomorphological and sedimentological insights to reconstruct past floods: Insights from Kea Point, Mt. Cook Village, Aotearoa New Zealand, *Geomorphology* (2021), <https://doi.org/10.1016/j.geomorph.2021.108028>

This is a PDF file of an article that has undergone enhancements after acceptance, such as the addition of a cover page and metadata, and formatting for readability, but it is not yet the definitive version of record. This version will undergo additional copyediting, typesetting and review before it is published in its final form, but we are providing this version to give early visibility of the article. Please note that, during the production process, errors may be discovered which could affect the content, and all legal disclaimers that apply to the journal pertain.

**Integrating historical, geomorphological and sedimentological insights to reconstruct past floods:
insights from Kea Point, Mt Cook Village, Aotearoa New Zealand**

**Williams, R.D.^{1*}, H.M. Griffiths², J.R. Carr³, A.J. Hepburn², M. Gibson², J.J. Williams⁴, T.D.L. Irvine-
Fynn²**

¹ School of Geographical and Earth Sciences, University of Glasgow, Glasgow, G12 8QQ, UK.

² Department of Geography and Earth Sciences, Aberystwyth University, Aberystwyth, SY23 3DB. UK.

³ School of Geography, Politics and Sociology, Newcastle University Newcastle upon Tyne, NE1 7RU, UK.

⁴ Department of Social Sciences, Oxford Brookes University, Headington Campus, Oxford, OX3 0BP. UK.

* Corresponding author, richard.williams@glasgow.ac.uk

Key Points

- Glacial lake outburst floods occurred in January and March 1913
- Floods eroded lateral moraines and roads to the original Hermitage Hotel
- Written documentary records provide detail on flood source, pathway & receptors
- Integrated approach enables cross-validation of insight from individual resources
- A generic reconstruction framework shows the utility of different resources

Key words

Glacial lake outburst flood (GLOF), flood reconstruction, Structure from Motion (SfM) photogrammetry, Aotearoa New Zealand, historical evidence, palaeoflood evidence.

1. Introduction

1.1 Reconstruction of past floods

Natural hazards represent an ongoing threat to human activities and infrastructure, and have an increasing societal cost (Cutter et al., 2015; Hyndman and Hyndman, 2017). Management strategies for natural hazards typically depend on being able to delineate risk zones based on knowledge of a particular hazard's occurrence, magnitude, frequency and temporal dynamics. Such information can be obtained through the reconstruction of geohazard events. As illustrated by work on flooding, various historical, botanical and geological archives may provide valuable information for these reconstructions (Wilhelm et al., 2019). Despite this wide range of datasets, previous reconstructions of floods, and other geohazards, tend to rely on archives from individual disciplines. Therefore, developing multi-archive approaches and frameworks to reconstruct paleo- and historical floods is desirable (Agatova and Nepop, 2019; Schulte et al., 2019b; Zaginaev et al., 2019; Schulte et al., 2020).

Historical documents and artefacts have been used extensively in geomorphological research, with sources including: discharge records; epigraphic records; aerial and ground-based oblique photographs; litter; climate records; land-use surveys; and written descriptions and accounts (Hooke and Kain, 1982; Brazdil et al., 2006; Trimble, 2008; Wetter et al., 2011; Grabowski and Gurnell, 2016). The uncertainties, and spatial and temporal coverage, associated with each dataset vary, and so the combined use of multiple sources increases the accuracy and validity of reconstructions. For example, sources written by non-specialists (e.g. newspaper and periodical articles and books) may be less quantitative than scientific articles, but can nevertheless yield useful additional context, if appropriate caveats are considered (Trimble, 2008). As a result, historical newspaper articles have been used to successfully determine records of flooding (Jeffers, 2014), channel migration (Kemp et al., 2015) and mass movement (Taylor et al., 2015). In recent years, the development of free, online, searchable digital archives has facilitated the use of regional historical newspapers for the

construction of natural hazard databases (Jeffers, 2014; Foulds et al., 2014). Thus, previous work demonstrates the utility of historical documents in reconstructing floods, including non-specialist sources.

Evidence for past flood characteristics can also be determined from sediment signatures, if high flows are connected to sediment sources, and from topographic signatures, if floods cause reworking of the channel geometry (Carling, 1986; Cenderelli and Wohl, 1998; Harrison et al., 2006; Breien et al., 2008; Westoby et al., 2014; Vilimek et al., 2015; Jacquet et al., 2017; Kougkoulos et al., 2018; Nie et al., 2018). Fluvial sedimentary deposits can include both coarse material mobilised under, and deposited immediately following, peak discharge (Kershaw et al., 2005), and fine material deposited during waning flow or inter-flood discharges (e.g. Marriott, 1992). Both catchment configuration and sediment availability influence the spatial distribution of sediment deposits but where channel, channel margin or overbank deposits are available they can provide a rich resource for determining the age of flood events (e.g. Elv et al., 1992; Macklin et al., 2012). If coarse sediment is transported by a flood, then measurements of isolated boulder deposits in the flood channel can be used to reconstruct flow velocity and discharge using empirical techniques (Costa, 1983; Williams, 1983). The slope-area method (Peggs, 1976; Williams, 1978) and hydraulic modelling (e.g. Cenderelli and Wohl, 2001) can also be used to reconstruct minimum flood magnitudes from cross-sectional geometry and high-water mark deposits or markers. Although sedimentary and topographic signatures provide valuable information on flood magnitudes, there are considerable uncertainties. These uncertainties can be reduced, and flood characteristics better constrained, through incorporation of data from other sources (Kershaw et al., 2005; Lumbroso and Gaume, 2012). However, few studies have fully integrated these historical sources with geomorphological and sedimentological evidence.

1.2 Glacial lake outburst floods in mountain environments

Recent climate warming (Yan et al., 2016) has enhanced environmental change and its associated risks in mountain environments (Beniston, 2003; Marston 2008; Viviroli et al., 2011; IPCC, 2019; McDowell et al., 2014). Natural hazards in mountainous regions result primarily from large-scale mass flows comprising rock and ice avalanches, glacier-derived meltwater and seismically-, volcanically- or thaw-driven releases of material (Slaymaker, 2010). Furthermore, glacier recession and elevated ablation, coupled with potential for formation of coalescing supraglacial ponds, can promote the formation of ice-marginal and/or proglacial lakes, commonly impounded by moraine ridges (e.g. Benn et al., 2012). In certain circumstances, such lakes may rapidly drain, causing a glacial lake outburst flood (GLOF; Clague and Evans, 2000; Richardson and Reynolds, 2000; Frey et al., 2010; Clague et al., 2012; Westoby et al., 2014; Haeberli et al., 2017). GLOFs can be triggered by a number of factors, including: failure of a barrier; inputs from landslides, rockfalls, iceberg calving and/or avalanches; seismic activity, and/or rapid water inputs (e.g. Richardson and Reynolds, 2000; Westoby et al. 2014, 2015; Rounce et al., 2016). GLOF incidence may increase in the future in some regions, as climate warms and glaciers retreat, resulting in larger meltwater volumes and, in some cases, the formation and expansion of glacial lakes (Carrivick and Tweed, 2016; Hock et al., 2019; Shugar et al., 2019). Critically, not all ice-marginal or proglacial lakes are hazardous (Frey et al., 2010) and in cases where glaciers recede far beyond their Little Ice Age (LIA) maxima, lakes or overdeepenings may not be distant from unstable glacier margins and active mountain slopes. Furthermore, a direct link between climate forcing and GLOF triggering or frequency has not been established (Harrison et al., 2018; Veh et al., 2019). Thus, despite the rapid increase in GLOF research, significant gaps remain in our current knowledge of their triggering mechanisms, progression and societal impacts. One approach to addressing this knowledge gap is to reconstruct past events (e.g. Wilson et al., 2018), which allows us to understand the GLOF event as a whole, including its driving mechanisms, environmental and social impacts, and public perceptions of past occurrences.

1.3 Aim and structure

We use an integrated approach to examine an historical natural hazard event observed in the Aoraki Mount Cook region of Aotearoa New Zealand in 1913, where heavy rain caused waters from Mueller Glacier to overtop the moraine at Kea Point (Figure 1; Figure 2). This event destroyed the original Hermitage Hotel (Figure 2D) and for which a rich documentary archive exists. Our aim, here, is to reconstruct the GLOF by integrating historical archival materials, that provide insight into the timing and spatial impact of the GLOF, with geomorphological and sedimentological analyses to provide information about processes of the GLOF itself. Our results are presented in the style of a source-pathway-receptor model (Holdgate, 1979); source refers to the origin of floodwater, pathway to flood routing and receptor the impact of the flood in terms of geomorphic change and damage to people, property and/or infrastructure. Evidence is collated from different sources, and employed to reconstruct the GLOF trigger(s), timeline, peak discharge, geomorphological impact, and consequences for people and property. The discussion (i) evaluates the insight gained from integrating interdisciplinary data, (ii) identifies limitations and how other datasets could augment the reconstruction and (iii) develops a framework summarising how different observational and archival sources can be used to reconstruct different phases of flood events.

2. Study Area

Aotearoa New Zealand's South Island (Te Wai Pounamu), is dominated by the Southern Alps (Kā Tiritiri o te Moana), which trend southwest-northeast for ~600 km with peaks ~2000 m. Oriented perpendicular to the prevailing mid-latitude westerlies, the orographic influence results in an annual precipitation regime characterised by a steep across-range gradient, with < 5 m/year to the west, around 12–15 m/year in the mountains, and c. 1 m in the eastern rain-shadow edge of the range (Mosley and Pearson 1997). Extreme rainfall events are not uncommon, particularly over the alpine range, with individual synoptic storms delivering 7 to 20 mm/hr over 1- to 5-day periods (Whitehouse, 1982; Henderson and Thompson 1999). At elevations above 1500 m a.s.l., air temperatures remain below 0°C for > 27% of the year (Hales and Roering, 2005). The high

precipitation regime and low winter temperatures promote glaciation in the Southern Alps. Over the last 7 ka, these glaciers have undergone numerous advance and recession cycles (Gellally et al., 1985; Schaefer et al., 2009) and from the late 19th century, they have retreated (Chinn et al., 2014; Carrivick et al., 2020): ice volume was estimated at 170 km³ in 1850 (Hoelzle et al., 2007), shrinking to 46 km³ in 2008 (Chinn et al., 2012). Recent New Zealand glacier recession is dominated by 12 large lake-terminating glaciers, which account for 71 % of ice loss between 1976 and 2009 (Chinn et al. 2014). Due to the contemporary presence of the large proglacial lakes, these 12 large glaciers are now largely decoupled from climate and have slow response times (Chinn et al., 2014).

The Mueller Glacier is one of these 12 large lake-terminating glaciers and has shrunk dramatically since the Little Ice Age (LIA; Figure 1 and Figure 2), which is estimated to have occurred between ~1450 and 1850 CE in the Southern Alps (Lorrey et al., 2011). Much of the glacier ablation area is covered in rock debris, which has resulted in uneven surface downwasting, at rates of 0.5-1.2 m/a since ~1900 (Burrows, 1973, Robertson et al. 2012), and the formation of ice surface ponds (Kirkbride, 1993; Rohl, 2008; Figure 1 and Figure 2). These ponds have enhanced melting and coalesced, facilitating rapid growth of the proglacial Mueller Lake (Robertson et al., 2012), at rates of 130 m/year between 2000 and 2018 (Pelto, 2018). Mueller Lake formed from ~1900 and is enclosed by an arcuate moraine complex characterised by a series of nested ridges (Burrows, 1973; Barrell et al., 2011; Figure 1 and Figure 2), with maximum moraine ridge crest elevation ~120–150 m above the contemporary lake level (Allen et al., 2009). The series of ridges have been subject to a variety of studies aimed to resolve the processes and timing of their formation (Burrows, 1973; Gellally, 1984; Winkler, 2000; Schaefer et al. 2009; Kirkbride and Winkler, 2012; Reznichenko et al; 2016).

The shrinkage of Mueller Glacier and its tributaries has generated a number of on-going potential hazards (Allen et al., 2009): (i) the moraine height above the lake now approaches the threshold of stability particularly for high-rainfall conditions (Blair, 1994); (ii) active rockfalls arising from

debutressing periodically deliver material to the glacier surface from the surrounding mountain flanks (Allen et al., 2011; Cox and Allen, 2009; McColl, 2012; Cody et al., 2020); (iii) ice avalanches from the now disconnected hanging glaciers deposit on to the glacier terminus and may affect the associated moraine complex (Iseli, 1991); (iv) the likelihood of a large earthquake ($>$ Magnitude 7, Richter Scale) in the region before 2050 may be as high as 35 % (Cox and Barrell, 2007). Collectively, these hazards represent high-likelihood causes of Mueller Lake water outflow and subsequent downstream flooding and erosion to the south of Mount Cook Village (Allen et al., 2009). At the same time, tourist activity downstream of Mueller Lake has increased dramatically in recent years, with visitor numbers to the Aoraki Mount Cook National Park reaching one million for the first time in 2018 (DOC, 2019). Therefore, exploration of previous glacial flood events in the local area is important and timely.

3. Methodology

3.1 Historical resources

Historical documents that referred to the 2013 Kea Point outburst flood events were identified from a search in the National Library of New Zealand's database of digitised historical documents (Papers Past Website, 2020). Information related to antecedent conditions, timing, magnitude and impacts were noted, along with how the floods were portrayed and the type of style and language used based on critical source analysis (Himmelsbach et al., 2015). Information identified from this database was supplemented by material from Freda de Faur's *The Conquest of Mount Cook* (1915), internet searches, materials available from the Department of Conservation (DOC) Mt Cook Visitor Centre archive, and personal communications with experts in Aotearoa New Zealand glaciology (Table 1).

3.2 Geomorphology

A schematic geomorphological map (Figure 3) was built based on combining IKONOS-2 satellite images (acquired 22:34 11 April 2003) and existing moraine ridge age maps. Ground-based hand-

held Garmin eTrex GPS (horizontal precision ~ 3 m) observations were used to validate the key features identified within the satellite images. Moraine ridge chronology was defined by the ^{10}Be dates reported by Schaefer et al (2009). A high-resolution Digital Elevation Model (DEM) and an orthoimage of the breach site and the upstream 400 m of the outburst channel were produced using Structure from Motion (SfM) photogrammetry (Carrivick and Smith, 2019; Eltner and Sofia, 2020). Images were acquired on 11 April 2015, from a height of approximately 50 m above the valley floor using a DJI Phantom 2 Vision+ Unmanned Aerial Vehicle (UAV) with an integrated 14 megapixel camera. Forty-seven targets were distributed across the 0.13 km^2 survey area. A benchmark was installed within the survey area and observed in Global Navigation Satellite System (GNSS) static mode using Leica 1200 series survey equipment mounted on a tripod. The position of the benchmark was subsequently post-processed using RINEX data from PositionNZ's nearest (43 km) permanent GNSS station at Mt John Observatory. Targets were subsequently observed using Real Time Kinematic (RTK) GNSS observations with a Leica 1200 series antenna mounted on a 2 m pole that was positioned in the centre of each target. Coordinates were transformed to the New Zealand Transverse Mercator 2000 (EGM96 geoid) coordinate system and the New Zealand Geodetic Datum 2000. Widely used Pix4D software (e.g. Bakker and Lane, 2017; Stott et al., 2020), was used for SfM photogrammetry. The rolling shutter effect from the Phantom 2 Vision+ camera was corrected by modelling the rolling shutter's rotation and translation effects (Vautherin et al., 2016). Twenty-two targets were identified as Ground Control Points (GCPs) and were used to scale and georeference the point cloud. The remaining 25 targets were used as Ground Validation Points (GVPs) to evaluate the Root Mean Square Errors (RMSE) of the point cloud, which were 0.032, 0.042 and 0.032 m in the x, y and z dimensions respectively. The output DEM and orthomosaic had a 0.1 m horizontal resolution (Figure 4).

3.3 Sedimentology

A total of 843 exposed clasts were sampled randomly throughout the flood reach, with location recorded using a hand-held Garmin eTrex GPS and A-, B- and C-axes measured with an uncertainty of ~ 0.01 m. Data were collected on 17 April 2014, by five observer groups, who all received identical training and were audited at the start of data collection to minimise measurement inconsistencies. Based on clast measurement location we identified three major assemblages: (1) the main outburst flood channel, (2) moraine clasts, as comparative data, sampled close to the breach point, and (3) clasts suggestive of a channel braid to the West of the valley floor and flood thalweg. The moraine dataset was collected from the Mueller Glacier's moraine surface immediately to the North-West of the Kea Point breach, following the orientation of the local ridge- and gulley-lines. Orientation of all clasts' A-axis was measured relative to South, between -90° and 90° (respectively, West to East) to within $\pm 3^\circ$. Roundness was assessed visually and subjectively according to the categorical Power's Roundness Index from Very Angular (VA) to Well Rounded (WR) indicative of the degree of erosion that boulders had likely experienced. To assess the origin of each boulder, Relative Angularity (RA: percentage of angular and very angular clasts) and C40 (percentage of clasts with C/A axial ratio ≤ 0.4) indices were also calculated for groupings of clasts based upon their assemblage classification or longitudinal geographic distribution. Facies envelopes plotted on a covariate plot of the RA and C40 indices (Benn and Ballantyne, 1994) to guide interpretation.

To interrogate these data further, we described the flood path using a fourth degree polynomial fitted through the measured 'channel' clast locations (Figure 5a). This yielded a notional flood thalweg, with a flow length of 1730 m limited by our observations. At 12.5% intervals along this thalweg, 110 m radius zones were employed to subsample the data to assess downstream variations in sediment characteristics at the reach-scale; the selected radius provided the greatest subsampling coverage and minimal overlap between zones. This approach only excluded 43 clast records from the flood channel observation set. Using a sedimentological approach to the paleoflood (Section 3.4.2) for each sample reach along thalweg we derived a flow velocity using the "intermediate

diameter” (B-axis) of the largest five clasts and discharge was estimated using the “nominal” diameter (A-axis; following Costa, 1983; Kershaw et al., 2005).

3.4 Discharge reconstruction

3.4.1 Rainwater volume estimation

In the absence of detailed glacier topography and meteorological data for 1913, simple glacial and hydrological modelling was used to estimate the historical Mueller Glacier catchment area. This was used to provide a first order approximation of the rainfall volume contributing to the outburst flood. To reconstruct Mueller Glacier, the bed topography was estimated using the ‘extended perfect plasticity’ method (Li et al., 2012). The estimated ice thicknesses, together with the elevation of contemporary glacier-adjacent terrain (LINZ, 2019), were combined using the MATLAB RegulariseData3D function to generate an ice-free topography in the (currently) glacierised catchment at 100 m resolution. The ArcGIS Glacier Reconstruction (GlaRe) toolset (Pellitero et al., 2016) was then used to generate an approximated bare-ice glacier surface from a central flowline using a 2D perfect-plasticity central reference model (Benn and Hulton 2010). The model initialisation point at the glacier terminus was defined from historical imagery from 1904, when the terminus was ~ 100 m from the LIA moraine (Figure 3). However, owing to the model resolution, the geometry of the reconstructed glacier above Kea Point was insensitive to the absolute glacier margin position within the range of positions delimited by the recent (c.100 years BP) ice margin and the LIA moraine ridges. The relatively coarse resolution of 100 m and a bare-ice approximation were chosen to describe the former glacier’s approximate geometry. While historical records indicate debris-covered portions of the lower glacier and, for example, an ice-marginal pond at the location that became the Kea Point moraine breach (du Faur, 1915), our modelled glacier surface geometry does not account for such features since defining a finer resolution topography would be speculative. Having modelled the approximate extent of the Mueller Glacier in 1913, we then reincorporated this output into the contemporary DEM to provide an estimate of the former catchment area at the time

of the outburst floods. The ESRI ArcGIS Hydrology toolset was used to calculate a contributing catchment draining to the breach location and this area was coupled with the historical rainfall data, to define a potential pluvial runoff amount. A zero-lapse rate in precipitation across the catchment was assumed (see Kerr et al., 2011), and the estimated water volume excludes the effects of ice melt or rainfall retention in snow-covered areas at higher elevations in the catchment. Accordingly, this approach simply provides a first order value to compare with geomorphologically-derived discharge estimates.

3.4.2 Sedimentological and topographic approach

Instantaneous peak discharge was estimated using slope-area and boulder measurement empirical regression equations (Table 2). Slope-area methods assume uniform flow and constant cross-sectional geometry along a reach. Further, because there is a relation between channel roughness and water-surface slope in natural channels, slope-area methods assume that longitudinal slope replaces a roughness coefficient and hydraulic radius is related to cross-sectional area. To apply slope-area methods, geometric and longitudinal slope inputs were extracted from the SfM photogrammetry DEM at four representative cross-sections that were positioned at the breach point and along the upstream portion of the outburst channel (Figure 4). The boulder measurement approach uses a nominal sediment particle diameter for each cross-section discharges were calculated for the ten particles that were located closest to the cross-section; this meant that no particle was more than 10 m upstream or downstream from the cross-section. Uncertainty in this empirical approach is widely recognised (Kershaw et al., 2005) but nevertheless gives a first order approximation of peak discharge (Q_p).

4 Results

4.1 Conditions antecedent to the Kea Point flood

Prior to the outburst floods, there was a subtle depression in the southern moraine ridgeline at Kea Point that was thought to have resulted from minor ice incursions and meltwater spillover or seepage during the mid-1700s and mid-1850s glacier advances (Burrows 1973). While ice surface elevations were high in the late 1800s, during enhanced melt or heavy rainfall events a small portion of runoff from the glacier surface drained from the Mueller Glacier exploiting the Kea Point topographic low (Ross, 1893; Marshall, 1907) resulting in the likely ephemeral occupation of a channel path on the southern side of the moraine complex (Figure 3). du Faur (1915, p. 213) noted that at the topographic low at Kea Point, a small lake “usually only a few feet deep” was impounded by the geometry of the glacier surface and moraine. In 1913, two main floods occurred: the first in late January and the second in late March. The latter destroyed the original Hermitage Hotel (Figure 2D). Debris from the moraine was reworked through a narrow chute, forming an alluvial fan between the LIA moraine and Mt Ollivier (Figure 6).

4.2 The triggering event

4.2.1 January 1913

The first newspaper reports of the January flood appear on the 21st of the month in a syndicated report in the Poverty Bay Herald, Ashburton Guardian, the Evening Post, and the Green River Argus (Figure 5). This observation, written, according to the title of the piece, on Monday 20th January, notes that “for the past eleven days heavy rain has been experienced” at the Hermitage and that “On Sunday, there was an exceptional downpour” (Poverty Bay Herald, 1913a, p. 3). This suggests that a period of rainfall had begun on the 9th January (Figure 7). du Faur (1915) confirms this extended period of rainfall but suggests that it had been falling for a longer period. du Faur, a mountaineer, and two guides had achieved the first complete traverse of Mount Cook on the 3rd January and had returned to the Hermitage Hotel on the afternoon of the 4th January. She states that “...the weather turned bad the day after our return from Mount Cook” (du Faur, 1915, p. 209), suggesting the 5th January, and “for ten days the rain came down steadily...” Later, waiting for good

weather to attempt a second ascent of Mount Cook, she says “For sixteen days we never saw the sun; the first fourteen it rained steadily day and night, but the last forty-eight hours it came down in solid sheets, each drop seemed to contain a bucketful” (de Faur, 1915, p.210). Assuming that it had begun raining on the 5th January, fourteen days of rain takes us to the 19th January, with the “last forty-eight hours” being the 19th January when the first flood occurred, and the 20th January, which saw continued flooding (Figure 7). du Faur describes the sustained antecedent rainfall as “a warm rain that had melted snow in all directions” (p. 213). A subsequent report in the Timaru Herald on the 23rd January notes that the flood occurred on Sunday the 19th January around “4 or 5 o’clock, after a torrential rain had been falling for three days” (Timaru Herald, 1913a, p. 5). This first flood seems to have been caused by approximately two weeks of sustained rainfall, with 2-3 days of particularly intense rainfall between the 18th and 20th January (Figure 7). This was confirmed by other reports in the Timaru Herald, of “exceptionally heavy downpours on Saturday and Sunday” (Timaru Herald, 1913b, p. 4) and a letter in the same paper saying “After 10 days of continuous rain over the ranges and valleys about Mount Cook, the wet weather culminated on Sunday afternoon in a torrential downpour, with lightning in the night and a heavy gale. This lasted without intermission all night and during Monday until the evening” (Timaru Herald, 1913c, p. 3).

4.2.2 March 1913

On the 29th of March the Ashburton Guardian, the Colonist, the Grey River Argus, and the Hamera and Normanby Star carried a syndicated report, written on 28th January. This stated that “ten inches [of rain; 254 mm] have fallen in 22 hours, and the gauge was then submerged” (Ashburton Guardian, 1913, p. 5). Another syndicated press report issued on the 28th of March notes “Up to nine o’clock yesterday morning 983 points [9.83 inches; 250 mm] of rain had fallen and it rained heavily all day. After this a further six inches [152 mm] fell up to 9.30 last night, ...” (Press, 1913a, p. 12; Timaru Herald, 1913d, p. 9). Another report notes that 19 inches [483 mm] of rain fell in 48 hours (Star, 1913a, p. 7). The Press report also states “there was a nor’-west wind in the morning” and “The rain

came from the same direction as the one which caused such a serious flood in January last..." (Press, 1913a, p. 12). Other reports describe widespread flooding across New Zealand in March 1913 (Star, 1913a). Once again, mention is made of the "unusually wet" (Press, 1913a, p. 12) weather which had persisted for three months at Mount Cook and that the rivers were fed by "snow melted by warm rains in the back country" (Oamaru Mail, 1913, p. 4). The Press (Press, 1913a, p. 12) reports that a "torrential downpour ... set in last Thursday morning." Some reports describe that less rain fell than in January, and that it was not as heavy, but that it was a longer period of rainfall (Timaru Herald, 1913e, p. 8). In contrast, another report in the Press, states "The rain came from the same direction as the one which caused such a serious flood in January last, but the present one is more severe" and "13 inches [330 mm] higher" (Press, 1913a, p. 12). Whitehouse (1982) estimated that the return period of this storm was 250 years.

4.2.4 Discharge estimation

Using available data and a combination of simple glacier and hydraulic modelling, the potential rainfall volume that contributed to the March Kea Point outburst flood was estimated. Historical accounts indicate 9.8 inches [249 mm] of rain fell over 23 hours during the most intense period of rainfall (section 4.2.2). From the assumed glacier geometry, the total volume of rainfall which fell within the $\sim 39 \text{ km}^2$ watershed (figure 1) over 23 hours was estimated to be ~ 9.7 million m^3 . If this pluvial input translated to a flood event over the same timeframe, crude estimates can be made of a constant discharge of $\sim 120 \text{ m}^3 \text{ s}^{-1}$, or for a peaked hydrograph reaching $\sim 230 \text{ m}^3 \text{ s}^{-1}$. In the absence of more detailed glacier surface topography and hydrological characteristics, and local meteorological data from 1913, this first-order estimate of rainwater volume is a useful means of approximating potential discharge magnitude and contextualising instantaneous peak discharge estimates derived from the sedimentological and topographic approaches.

Figure 4 shows the locations of four cross-sections that were positioned along the pathway of the Kea Point GLOF to provide topographic data to estimate instantaneous discharge. XS1 is located at

the breach point, XS2 is located 25 m farther downstream, and XS3 and XS4 are located along the course of the GLOF. Table 3 lists the peak discharge estimates at each cross-section, using slope-area and boulder measurement approaches. Discharges estimated using the three slope-area approaches vary by a factor of two for each cross-section. From all the methods at the four cross-sections, the minimum peak discharge was $316 \text{ m}^3\text{s}^{-1}$ and the maximum peak discharge estimate was $1077 \text{ m}^3\text{s}^{-1}$. Whilst the range is substantial, these estimates do give insight into the magnitude of the peak GLOF discharge. The standard deviations for the boulder measurement approaches are relatively large, caused by the range of sampled grain sizes (Figure 5). However, except for XS2, the mean peak discharge estimates are within the range that were obtained from the slope-area approach. Discharges estimated using the boulder measurement approach at XS2 were higher than the slope-area method. This may be due to the position of this cross-section close to a steepening of the longitudinal GLOF gradient (Figure 4), resulting in the erosion of finer clasts from this area and leaving a lag deposit of boulders that could not be entrained by the GLOF. Since there were two GLOFs, the complete timeline associated with moraine-sourced clast exposure and transport is unknown, and deposits may be superimposed. The instantaneous discharge estimates are, of course, greater than the volumetric estimation of an invariable flood discharge ($120 \text{ m}^3\text{s}^{-1}$); this, and comparison of their relative magnitudes, however, indicates that some confidence can be given to the overall estimated range of instantaneous peak discharge.

4.3 Reconstructing the GLOF timeline

4.3.1 January 2013

Water broke through the lateral moraine of the Mueller Glacier at Kea Point, with first peak outflow discharge occurring shortly after 4 pm on 19th January (Figure 7) and press reports recognised this as an outburst flood. For example, the Press Association Report says, “a rush of water came suddenly from the Mueller Glacier through an old breach in a moraine towards Kea Point” (Poverty Bay Herald, 1913b, p. 2) and “the surplus water from the Mueller Glacier came down with great force

about four o'clock" (Timaru Herald, 1913b, p. 4). In a letter to the Timaru Herald, a correspondent wrote, "On Sunday evening the Mueller river burst up through the glacier, and, breaking through the moraine, came down in a roaring torrent, past the Hermitage" (Timaru Herald, 1913c, p.3). de Faur (1915) writes: "the Muller (sic) river was coming down Kea Point (p. 210) and 'we beheld a yellow flood coming straight at us' (p. 210)". The rains continued, and a report in the Timaru Herald noted "A weak part of the lateral moraine of the Mueller glacier was broken through by the flood waters and an enormous stream issued from the ice at the side of the glacier. This increased in volume as the night wore on" (Timaru Herald, 1913a, p.5).

A second peak outflow discharge occurred in the early hours of 20th January (Figure 7). du Faur wrote "Some time in the dim hours of the early morning I was awakened by a terrific crash... the water was flowing under the front door" and "the roar that had waked me was the grinding together of a great mass of boulder swept down from the Mueller moraine" (p. 211-12). Around half an hour after dawn, "the water began receding slowly but steadily, and as no more moraine came down the danger was over for the time being" (p. 212). Exploring the site later, du Faur describes the breaching of the moraine in detail, following increased water levels in the lake behind - "conditions caused the lake [at Kea Point], which receives a large portion of the drainage of the Mueller moraine, to rise about 20 feet, when the pressure of the water burst the bank of the moraine separating the lake from the valley" (du Faur, 1915, p.213), and the moraine breaking due to increased pressure: "Above the lake the sides of the next wave of moraine were washed to a clear wall of ice through the cracks of which water was gushing in every direction; but the main stream came from round Sealy Point and was the drainage from the head of the glacier" (p. 213-4). Another report notes that the Mueller moraine had collapsed near the point where the Hooker issues, causing a portion of the river to be diverted into another course (Lyttelton Times, 1913). Crucially, two reports note that the flood issued through an historic breach in the moraine "where flood waters had evidently broken through at some previous time" (Timaru Herald, 1913f, p. 5) and another notes that this was a "weak part of the lateral moraine" (Timaru Herald, 1913a, p.5).

4.3.2 March 1913

Compared to the information regarding the January event, fewer details are available about the nature and timing of the March event (Figure 7). A syndicated report notes that the flood issued from the breach in the lateral moraine: “Generally the flood comes from the Mueller glacier through a gap in the old side of the Moraine and this time chunks of ice are coming away with the boulders” (Wanganui Chronicle, 1913, p. 5). Another report states that “the Hooker commenced to rise on Friday morning” and “By three o’clock the river was a roaring torrent, carrying huge boulders and masses of ice” (Oamaru Mail, 1913, p. 4). The presence of these masses of ice suggests that the flood event occurred on the afternoon of the 28th of March. Moreover, another report describes how the river had breached the terminus of the Mueller glacier, rather than the lateral moraine – “The ice caves where the river rushes out from the terminal face of the Muller Glacier had disappeared. The flood swept through a gorge of solid ice, the walls of which rose to a height of 100 feet” (Poverty Bay Herald, 1913c, p. 5). It is, therefore, likely that in March the floodwaters arose from flows that breached both the terminal and lateral moraines of the Mueller glacier. The breach point at Kea Point may have been enlarged by further erosion of the January flood spillway and residual ice-cored moraine or a downwasting ice margin. By inference, the records also suggest that an in spate Hooker River, flowing South from the Hooker Glacier and draining through the terminal region of the Mueller Glacier, caused the collapse of ice bridges above the usual en- or sub-glacial drainage channels, and consequently, enlarged the drainage pathways through the terminal region of the Mueller Glacier, and further incised the proglacial drainage to the South East of the moraine complex (Figure 7).

4.5 Geomorphological impact

4.5.1 January 1913

Geomorphological impacts of the January 1913 flood were well-described by du Faur (2015) and in selected newspaper reports (Figure 7). The flood transported very large volumes of boulders (Figure

6). du Faur describes “a great mass of boulders swept down from the Mueller moraine and deposited not ten yards from the front door” (p. 212) and as the flood subsided describes “a waste of grey, water-worn boulders of every shape and size” (p. 215) before the hotel. This is confirmed by a Press Association report which states that the flood had “covered a large area with big boulders” and another noting that the rivers were “rolling down heavy boulders” (Hawera and Normanby Star, 1913, p. 5). According to du Faur the flood also transported “shrubs, uprooted trees” (p. 210), “blocks of ice” and “moraine” (p. 213) (taken to mean boulders and other sediment). A correspondent also talks of “trees and large boulders” being carried, with the boulders being deposited against fences, or causing them to be destroyed and “strewn rocks over about an acre of grass land” (Timaru Herald, 1913c, p. 3). A report in the Timaru Herald calls this “a huge temporary moraine” (Timaru Herald, 1913b, p. 4). The reports also described the flood eroding new river channels. du Faur describes the flood splitting in two at the front gate of the hotel, with the main flow directed down the road and a smaller flow directed towards the hotel. This smaller stream subsided towards the evening, with the main flow continuing to flow down the road. du Faur notes that this new river ‘had already cut itself a channel half as big as the Hooker’ (p. 213), which would have been ~200m, based on descriptions of the Hooker from later reports in March, and her descriptions of having to be carried over “side streams” (p. 213) suggests that the flood had formed a multi-thread planform. As the flood subsided, du Faur describes how the river had “dwindled to a tiny stream flowing between the high banks” (p. 215).

4.5.2 March 1913

Compared to the January event, more detailed descriptions exist of the geomorphological impacts of the March event, and these suggest that the March flood was of greater magnitude (Figure 7). Significant impacts were described at the terminal face of the Mueller Glacier: guides observed “great avalanches of ice weighing hundreds of tons came toppling across the stream with a thundering crash...scattering the rocks and shingle of the moraine in all directions, and making a

dam through which the water burst with a terrific roar” (Poverty Bay Herald, 1913c, p. 5). Similar to the January event, very large pieces of ice and boulders were transported by the flood, variously described as “huge” (Poverty Bay Herald, 1913c, p. 5), “great” and “of immense size” (Star, 1913a, p. 7) (Figure 4). The blocks of ice were described as being “fifteen feet every way” (Press, 1913b, p. 4) and “20 ft wide” (Star, 1913a, p. 7) which were “hurled, tossed, up-ended and swept down the river” (Press, 1913b, p. 4). Once again, boulders were deposited in front of the Hermitage (Star, 1913a, p. 7). One vivid description explains how “the press of ice and boulders in the channel was such that huge stones and fragments of ice were shot out by the pressure above the highest flood marks, where they were seen next morning” (Oamaru Mail, 1913, p. 4) suggesting the deposition of perched boulders. Significant changes to river channel dimensions were also observed, particularly widening of the channel of the Hooker River – “...the river bed, which last week was a quarter of a mile wide, now extends for half a mile or more from side to side” (Press, 1913b, p. 4) (Fig. 4). One report describes how the flood in front of the Hermitage “gradually spread out over a larger area, and eventually cut such a channel as enabled it to get away more rapidly in another direction” (Press, 1913a, p. 12). This report also describes how the debris transported by the flood was “lodged in the channel cut by the rushing waters” (Press, 1913a, p. 12).

4.5.2 Overall geomorphological impact

Geomorphological mapping indicates that the Kea Point outburst floods occurred on the western lateral moraine of Mueller Glacier and cut through the 1890 lateral moraine (Figure 3). It formed a comparatively narrow channel, before breaching the 1750 moraine and, potentially, the moraine formed in the late 1660s. The outburst floods expanded into a flat area, bounded by the White Horse Hill moraine complex to the north-east and the steep valley side to the south-west. This section of hillslope has two large alluvial fans, which flow into the estimated flow path of the outburst floods.

The entire set of clast measurements are shown in Figure 5, with a summary given in Table 1. In general, the boulders showed a wide range of orientation from flow-parallel to transverse (Figure 5b), but with a greater propensity for more rounded boulders in the channel's mid-section (Figure 5c). Generally, the clast size decreased downstream, although with a large proportion of larger clasts at the lower deposit fan (Figure 5d-f). The descriptive statistics for the reach-scale variations in boulder metrics along the notional thalweg is shown in Figure 8. The reach-scale characterisation highlighted the similarity between the moraine and the boulders found both in the breach zone and on the lower downstream fan. In general the A-, B- and C-axis of boulders showed a similar downstream pattern: large boulders in the flood channel compared well to those in the moraine, assumed to be their source, although the boulder size between 400 and 1200 m along the notional thalweg was markedly reduced, suggesting contrasting flow conditions along the flood path. The palaeo-flood reconstructions are suggestive of peak velocities of $0.22\text{--}0.31\text{ ms}^{-1}$, and maximum discharges of $2680\text{--}10250\text{ m}^3\text{s}^{-1}$, according to the boulder sizes. However, the smaller boulders that characterise the mid-section of the flood channel, are far more rounded with a greater proportion of the SR and R classes (Figure 8f) and imply reduced reach-scale velocities and discharges, respectively, of only $\sim 0.15\text{ ms}^{-1}$ and $535\text{--}630\text{ m}^3\text{s}^{-1}$. Clast orientation was suggestive of some flow-parallel alignment, but notable proportions of near-flow-transverse deposition (Figure 8g). The RA/C40 ratio indicates that clast shapes were typical of moraine and glaciofluvial sediments (Figure 9). The moraine and braid clasts were broadly similar, although the moraine surface appeared to be slightly skewed to more rounded (SR) clasts. This was interpreted as a function of age of the moraine, and longer time-period for clasts to be exposed to subaerial weathering along the moraine ridge (cf. Figure 3). The Zingg diagram (Figure 9b) highlights the generally unremarkable shape of all clasts surveyed in this study, clustered around the boundaries between notional shape classes.

4.6 Impact on property and people

4.6.1 January 1913

The geomorphological consequences of the floods caused significant impact for the Hermitage hotel and tourists, particularly in terms of their ability to travel. A letter in a newspaper notes that the flood had eroded “a deep channel for itself along what had been the main road, quite obliterating it...” (Timaru Herald, 1913c, p. 3) with another report noting that the stream was “embedded with huge boulders and debris” (Timaru Herald, 1913b, p. 4). Many reports also note that damage, presumably erosion, had been done to the approaches to bridges (“sweeping and washing away the roads and approaches for some distance about the Hermitage” - Timaru Herald, 1913b, p. 4), although the bridges themselves remained undamaged with the exception of some of the footbridges.

4.6.2 March 1913

Erosion due to the March event led to damage of infrastructure, with a newly built bridge over the Hooker River being destroyed by the flood – “the ice blocks snapped the big piles like matches and the mad waters swept everything before them” (Press, 1913b, p. 4). A report also states that a rock “20 feet high and some 100 feet around its base, forming the support at one edge of the suspension bridge above the Hermitage, shifted nearly two feet” (Oamaru Mail, 1913, p. 4). Another bridge at Bushy Creek was “left dangling” (Press, 1913a, p. 12), roads and approaches to bridges were also destroyed and vegetation stripped away and transported downstream. Roads were “strewn with boulders and scoured out in deep ruts” (Press, 1913a, p. 12). Numerous new channels were cut into the land in front of the Hermitage Hotel – “The overflow from the Mueller Glacier turned many acres...into raging streams” and water “several feet deep” entered the hotel at four in the afternoon, causing a washhouse to be removed from its foundations (Star, 1913b, p. 4). The flood later caused the collapse of the front of the hotel into a stream which had a depth of “eight feet” (Star, 1913b, p. 4). Both events impacted significantly on tourist activities, to the extent that mention was made in a parliamentary paper (Tourist And Health Resorts Department, 1913, p. 4): “During January and the latter end of March record floods were experienced, doing considerable damage to the different

glacier tracks, and also washing away the Hooker cage and the whole of the structure of the new traffic-bridge over the Hooker River". A 'considerable amount of repairing-work' was undertaken, and the report notes that guiding work during the seasons reached record levels despite the damage.

5. Discussion

5.1 Insight gained from the integration of historical, geomorphological and sedimentological data

Focusing first on triggers, our results demonstrate that historical documentary data are valuable for reconstructing past flood events, and provide information that could not be determined from sedimentological or geomorphological evidence alone (Table 4). It is particularly useful where multiple sources can be used to triangulate information, and where the accounts are detailed. Specifically, written accounts can be used to determine event dates and the durations, and their temporal evolution, e.g. a piece in the Poverty Bay Herald on 20th January notes that "for the past eleven days heavy rain has been experienced" at the Hermitage and that "On Sunday, there was an exceptional downpour ..." (Poverty Bay Herald, 1913a, p. 3). The most useful reports are those that provide

specific quantities, e.g. "ten inches [of rain; 254 mm] have fallen in 22 hours, and the gauge was then submerged" (Ashburton Guardian, 1913, p. 5), but even descriptive data are helpful for identifying potential triggers e.g. "On Sunday, there was an exceptional downpour ..." (Poverty Bay Herald, 1913a, p. 3). Our documentary evidence provided useful broader context for the GLOF, by describing flooding across New Zealand (Star, 1913a), giving commentary on weather conditions that may have contributed the heavy rain, e.g. "there was a nor'-west wind in the morning" and comparing the event to previous floods "The rain came from the same direction as the one which caused such a serious flood in January last..." (Press, 1913a, p. 12). Finally, documentary evidence allows us to establish a direct link between triggers and the floods, which cannot be achieved with geomorphological or sedimentological data alone: the Timaru Herald (1913a, p. 5) noted that the

flood occurred on Sunday the 19th January around “4 or 5 o’clock, after a torrential rain had been falling for three days”. Thus, documentary data provided a wealth of information on the triggers of the Kea Point Flood that could not be determined from our other datasets.

Information on the breach point, breach mechanism and subsequent water flow paths was determined from a combination of documentary, geomorphological and sedimentological evidence (Table 4). For example, the large gap in the Mueller Glacier lateral moraine provides strong evidence for the location and dimensions of the breach point (Fig. 2), whilst clast and channel characteristics show the flood path and suggest that the clasts transported by the floods originated in the moraine (Figs. 2-3 & Figs. 5-6). The documentary evidence provides details on the breach, which is crucial for accurately modelling GLOFs, but is often poorly constrained (Westoby et al., 2015), e.g. du Faur notes “conditions caused the lake [at Kea Point] which receives a large portion of the drainage of the Mueller moraine, to rise about 20 feet, then the pressure of the water burst the bank of the moraine separating the lake from the valley” (du Faur, 1915, p.213). Furthermore, the documentary evidence allows us to construct a specific timeline for the flood e.g. “the surplus water from the Mueller Glacier came down with great force about four o’clock” (Timaru Herald, 1913b, p. 4) and how it progressed through time, e.g. “A weak part of the lateral moraine of the Mueller glacier was broken through by the flood waters and an enormous stream issued from the ice at the side of the glacier. This increased in volume as the night wore on” (Timaru Herald, 1913a, p.5). This can be integrated with information on downstream variations in clast size and distribution (Figure 6 and 7), to infer variations in flow along the flood path, particularly in areas lacking witnesses, e.g. close to the breach. The measured clast sizes mirror those reported in historical records to have been transported during the flood. Clast orientation provides detail on flow characteristics, with the varied clast orientation likely reflecting the complexity of depositional and transport mechanics in turbulent flow (Cenderelli and Wohl, 1998) during the floods. Our data suggest a transition from hyper-concentrated flow in the upper and mid-section of the channel to a debris flow in the lower section: results from the channels mid-section indicated reworking, which suggests that

concentrated flow close to the breach point exhumed and mobilised less-weathered, previously buried moraine materials and deposited them in this mid-section. In contrast, the lower degree of clast rounding both at the breach and the lower flood deposit fan (Figure 9) indicates that the floods behaved as a debris flow, mobilising sediment and moving large clasts across the fan (Pierson 2005; Calhoun and Clague, 2017). As such, sedimentological and geomorphological evidence provide useful information on flood flow paths, characteristics and evolution, and the breach characteristics, whilst documentary evidence allows us to place a timeline on these events, to validate clast sizes mobilised in the flood, to determine the event's evolution, and gain more detailed insight into the breach mechanism.

Valuable information on the geomorphological impacts of the Kea Point floods was gained from geomorphological mapping, through the identification of the Mueller Glacier moraine breach and flood pathways, and by quantifying the characteristics of clasts deposited by the floods (Figs. 2-4 & 6-7). The measured clast sizes and locations are broadly comparable to those reported in the historical record, with both datasets recording large boulders scattered through the channel cut by the flood and near the Original Hermitage Hotel. Together, this information can be used to infer the extent and broad-scale geomorphological impacts of the floods, which may not be well-represented in documentary evidence, as accounts may be more spatially constrained. It also provides an important opportunity to verify documentary evidence, to identify any potential bias or over / under exaggeration of the event. Documentary evidence allows us to attribute certain geomorphological impacts to a specific event and to separate the impacts of the January and March 1913 floods. Furthermore, documentary records provide information on more transitory geomorphological events that may not be recognisable in the geomorphological and/or sedimentary record, including: the formation of “a huge temporary moraine” (Timaru Herald, 1913b, p. 4), formed of trees and boulders; temporary changes in channel morphology and size, such as the widening of the Hooker River (“...the riverbed, which last week was a quarter of a mile wide, now extends for half a mile or more from side to side” (Press, 1913b, p. 4)); and ice avalanches, with guides observing “great

avalanches of ice weighing hundreds of tons came toppling across the stream with a thundering crash...scattering the rocks and shingle of the moraine in all directions, and making a dam through which the water burst with a terrific roar” (Poverty Bay Herald, 1913c, p. 5). Similarly, we can only indirectly infer impacts on humans and infrastructure from geomorphological and sedimentological evidence, for example by identifying infrastructure in the potential flood path, whereas documentary evidence can directly link human and infrastructure impacts to flood events.

Taken together, our case study of Kea Point highlights the utility of documentary evidence for reconstructing GLOFs, and floods more generally (Table 4). This is particularly the case for the flood source and receptors (Table 4). Whilst a number of paleoflood investigations have compared their data with historical flood series for calibration (e.g. Benito et al., 2004; Jones et al., 2012; Schulte et al., 2009), many only compare one archive with historical data. Studies that achieve spatial-temporal integration from more than one archive are comparatively rare (Schulte et al., 2015; Schulte et al., 2019a). Our investigation not only demonstrates how a range of archives can be mined to shed light on spatial-temporal dynamics of a historic flood but it also successfully applies this technique in a part of the world where there are comparatively few examples of multiproxy reconstructions (Schulte et al., 2019b). We recommend that future work makes use of documentary and digital (e.g. data from observers’ smartphones, cameras) information to reconstruct GLOFs as part of multiproxy reconstructions since documentary evidence can provide: important detail on key aspects of the event, such as the breach mechanism; a timeline for the event; data on transient features and impacts; and information on triggers and impacts that cannot be determined from the geomorphological record alone.

5.2. Limitations to the integrated approach and additional lines of evidence.

The various different methods used to reconstruct GLOF discharge broadly agreed (Table 3) but had a substantial range, in common with other investigations (e.g. Kershaw et al., 2005). If available, data from rainfall and discharge gauges would improve these estimates substantially. However, records

are not available for Kea Point, which is comparatively data-rich, and are unlikely to be available for other GLOF-impacted catchments, as they are often high altitude, remote and glaciated. Hydro- and morpho-dynamic numerical models can be used to reconstruct the pathways of floodwater, sediment flux and geomorphic change (e.g. Westoby et al., 2014; Staines and Carrivick, 2015; Williams et al., 2016), but these require substantial amounts of accurate input data to produce meaningful results. Our maximum discharge estimates based on boulder sizes are likely to be overestimates, due to the rapid variations in flow conditions that adjust transient impulsive forces and flow drag not accounted for (Costa, 1983) steady-state flow estimation (Alexander and Cooker, 2016). Furthermore, there is uncertainty over the origin and dates of the larger boulders further down the channel, which could be reworked older clasts and/or from paraglacial activity (McColl, 2012). Cosmogenic dating of these boulders would help to pinpoint their ages and hence to constrain our discharge estimates. Overall, we suggest that our range of discharge estimates is substantial, but we can take confidence from their broad agreement and comparison with pluvial water volumes; such estimates have utility in constraining potential GLOF magnitude, as well as augmenting information on the magnitude-frequency of GLOF events.

For Kea Point, detailed pieces of documentary evidence are plentiful, due to the site's history of tourism and comparative accessibility, which enabled us to construct a clear picture of the event (Table 1). Where rich and varied documentary archives are either related to one particular flood (e.g. McEwen and Werritty, 2007) or a specific location such as a city (e.g. Elleder et al., 2013) such evidence can be used to quantitatively reconstruct flood events. It can also sometimes be possible to use validate the accuracy of historical documentary records using geomorphological and hydraulic methods to reduce the uncertainty introduced by the limitations of the documentary approach (e.g. discontinuity, selective and subjective recording by individual and multiple recorders; Brázdil et al., 2006). The potential for such biases is potentially multiplied in a rich documentary context such as Kea Point where there are multiple, likely different recorders (e.g. du Faur and newspaper reporters) for the two flood events, each with individual perceptions, experience and writing styles. However,

many of the reports, including du Faur's journal and some of the syndicated newspaper reports are clearly first-hand accounts written immediately after (if not during) the events, and given that Kea Point experienced two flood events in relatively quick succession, more confidence can potentially be placed in the consistency of reporting between those two events. Although quantitative reconstruction of flood magnitude based on historical documents has not been possible here, the degree of agreement both between the various methods and the various historical sources on qualitative flood characteristics (flood type, nature of sediment movement, geomorphological impact) and the quantitative information in historical documents (e.g. rainfall volumes) illustrate the value of this integrated approach.

Documentary evidence elsewhere may be more limited and/or have a narrow spatial focus, particularly in more remote, sparsely populated areas. To supplement information from sparse documentary records, interviews could be conducted with those living in flood-prone communities and other types of knowledge (Wilkinson et al., 2020). This can provide rich material relating to impacts on people and landscapes and strategies to manage and adapt to flooding (McEwen et al., 2017). Similarly, triangulating between interviews and other datasets could help to resolve inconsistencies in documentary evidence, which we encountered in a small number of the Kea Point records. Although interviews with direct witnesses of events are limited to a maximum of ~80 years ago, valuable information can be gained via memories, oral traditions and folklore. Memories of flooding can be transmitted from generation to generation, provided that the floods or their impacts are of a certain magnitude (Griffiths and Tooth, 2020) and issues related to the accuracy of these memories can be overcome through integration of various types of data.

Our documentary evidence allowed us to reconstruct a detailed timeline for the Kea Point floods. For modern GLOFs that have occurred during the era of satellite remote sensing (Teng et al., 2017), radar and optical imagery may be available to reconstruct different components of a flood's source, pathway and receptors. On longer timescales, or where documentary evidence is scarce,

stratigraphic and biostratigraphic dating could be used to construct the timeline (Brown, 2011). For example, lichenometry, dendrochronology, radionuclides, tephrochronology, biostratigraphy and/or archaeology, could be used to constrain the timing of GLOFs and subsequent geomorphological activity. Finally, future work could draw on written records other than newspapers, report and letters, such as records of building repairs, cancellations of events or taxation records (e.g. Brázdil et al., 2014).

5.3 Framework for an integrated, multi-dataset approach to reconstructing GLOFs and other rapid onset floods

Table 5 details the types of data that can be used to reconstruct GLOFs and which datasets are most appropriate for reconstructing the various flood stages. Note that the range of resources extend beyond those that were used in this investigation. The range of potential datasets, and the types of information that they offer, will depend upon a variety of social and cultural factors, as well as physical factors, which will vary by place, country and time. For example, the availability of historical documents and artefacts will depend upon a society's norms for documenting, and archiving written work, and the transmission of this information to future generations may also depend on social and cultural factors (Griffiths and Tooth, 2020). The age, magnitude, spatial extent, geological and geomorphological context and magnitude/frequency of subsequent flood events are some of the physical factors that may influence the success of using documentary, sedimentological, geomorphological, and dating resources. Although not considered here, historical documents also offer a third utility, in that they are a window into historical and contemporary societal and cultural perceptions of extreme events (Griffiths and Salisbury, 2013; Jeffers, 2014; Griffiths et al., 2017). This provides important context on how people understand hazard and risk and, in turn, how this informs response. This information offers an important avenue for future research, both at Kea Point and in further developing the use of documentary data to reconstruct flood events, linking particularly with recent discussions regarding developing a 'critical physical geography' (Lave et al., 2014) and

proposed frameworks for engaging with indigenous peoples and their knowledge systems (Wilkinson et al., 2020). Schulte et al. (2019b: Figure 4) present a concept of multi-archive paleo-floodpaleoflood integration according to type of flood archive. It is notable that our investigation uses four (hydrology, historical sources, floodplain, landforms) of the ten archives that are identified in Schulte et al.'s conceptual model. Our framework (Table 5) extends the model further by considering which datasets are most appropriate for reconstructing various flood stages.

Societal and cultural perceptions and practices may also influence whether details are recorded in written records at all, and if they are, the type of detail. For the Koroit floods, the richness of the reconstruction is heavily influenced by the 'first person' reporting that was available from local newspapers and du Faur's (1915) book, both, in some ways, a result of the popularity of the area as a site of tourism. It is unlikely that the flooding would have been reported to such an extent had the original Hermitage Hotel, and the tourism industry not been impacted. This represents a challenge for reconstructing GLOFs elsewhere and requires us to consider other types of records that might yield useful information. Thus, our framework represents an overview and starting point for future work, which needs to be developed for specific physical, cultural and social conditions.

Contemporary written accounts and ground-based images and videos of floods published on social media are perhaps today's equivalents of the highly detailed, first-hand accounts utilised here. Such data have been widely used to reconstruct the spatial and temporal dynamics of flood events (Brouwer et al., 2017; Rosser et al., 2017; Wang et al., 2018; de Bruijn et al., 2019). Indeed, similar approaches are currently being used by Aoraki Mount Cook National Park to record the retreat of the Mueller Glacier, through uploads of tourist photographs from a fixed camera point at a popular tourist viewpoint. Thus, there is the potential to use this enormous archive of modern data to reconstruct recent GLOFs and those that may occur in the near-future. Although it is unclear to what extent these potentially rich resources will be archived for future analysis (Fondren and Menard McCune, 2018) compared to the established legal frameworks in place to archive printed media (e.g.

Feather, 2003), recent work has shown that large-scale analysis of such records can be undertaken (de Bruijn et al., 2019). Thus, the large volumes of data collected by the general public may provide a useful archive for reconstructing GLOFs in the future and also offers the opportunity for active engagement via citizen science.

6. Conclusion

Our reconstruction of the 1913 Kea Point outburst floods in the Aoraki Mt Cook region illustrates how a multi-disciplinary approach, triangulating information derived from geomorphological, sedimentological and historical resources, can elucidate flooding sources, pathways and receptors. Geomorphological analysis involved critical interrogation of existing academic literature, landform mapping from satellite imagery, fieldwork, and a high-resolution DEM and orthoimage that was produced using UAV imagery and SfM photogrammetry; this primary analysis was contextualised with published work on moraine ages. Sedimentological data included boulder size and location analysis, enabling an assessment of boulder origin and the direction of the floods' flowpath. Flood discharge reconstruction was undertaken using approaches based on first-order rainfall-runoff hydrological modelling (120 to 230 m³s⁻¹), a cross-section slope-area approach (316 to 1077 m³s⁻¹) using the SfM photogrammetry DEM, and boulder measurements (496 to 1622 m³s⁻¹). Whilst the peak discharge estimates vary, they provide context for the overall magnitude of the event. The historical resources explored here, including newspaper articles, a journal and parliamentary papers, revealed complementary information on antecedent conditions, flood sources, event timing and impacts. Analysis of these written records provided considerable detail for flood reconstruction; most significantly revealing that two glacial lake outburst floods had occurred. Our reconstruction strongly benefits from the relatively rich written record surrounding the original Hermitage Hotel, an iconic, newsworthy hostelry, due to the impacts of the January and March 1913 floods on the establishment, and the coincidence that a journal writer was staying at the hotel during the events. Combined, our evidential sources provide a coherent and reciprocally supportive qualitative and

quantitative narrative of the two flood events, their source, pathway and receptors. Today, the surface elevation of the contemporary Mueller Glacier is considerably lower than the crest of the moraine at Kea Point, so further GLOFs will not arise at this location during the current period of glacier mass loss. However, there remains the potential for outburst floods from Mueller Glacier lake from hydrological- or earthquake-induced landslides, ice avalanches from disconnecting hanging glaciers and rockfalls from debutressing, which may pose a risk to property and infrastructure along Hooker River. Nonetheless, the effective reconstruction of past geohazards is important for establishing magnitude-frequency relationships for contemporary risk assessments; this investigation not only reconstructs the Kea Point floods but also provides an illustration of how a multi-disciplinary, integrated approach can be used to yield a variety of information on an event that occurred over a century ago. Our proposed framework for such an approach to flood reconstruction, which considers both resources used in our investigation and those that may be available to other investigations elsewhere, highlights how historical documents and artefacts, sedimentological and geomorphological assessments, stratigraphic and biostratigraphic dating, environmental monitoring networks, numerical modelling and satellite remote sensing can and should be used informatively, consistently and simultaneously to shed light on a geohazard's source, pathway and/or receptors.

Acknowledgements

Fieldwork was funded by a British Society for Geomorphology (BSG) research grant to TDI, RDW and JRC. Aberystwyth University undergraduates on the 2014 and 2015 New Zealand South Island fieldtrips are thanked for field assistance. Thanks to Ray Bellringer (DOC Mt Cook) and The Hermitage Hotel who allowed access to archived materials and reports. Duncan Quincey processed satellite imagery. We also thank the late Trevor Chinn for providing us with photographs and expert knowledge of the field site, Craig MacDonell for producing Figures 1, and Lothar Schulte and Simon Cook for thorough reviews that strengthened this article.

Author contributions:

Conceptualisation (TDI and RDW); fieldwork (RDW, TDI, JRC, JJW, MG); formal analysis (HMG, JRC, RDW, TDI, AH); funding acquisition (TDI, RDW, JCR); visualisation (JRC, RDW, TDI); writing – original draft (RDW, JRC, HMG, AH, TDI); resources (RJC, TDI, HMG, RDW); all authors contributed to substantive reviewing and editing of the final manuscript.

Data

Sediment, orthoimage and topographic datasets that were produced as part of this investigation are available open access through the University of Glasgow's Enlighten digital data repository.

Figure captions

Figure 1 Study area setting, showing the location of the original Hermitage Hotel which was estimated from historic maps and photographs. Also shown is the estimated Little Ice Age extent of Mueller Glacier, based upon a coarse (100 m) resolution 2D perfect plasticity flowline model; small tributary glaciers are not represented in the model.

Figure 2. Annotated photographs of Kea Point and the surrounding area. (A) Location of Kea Point in relation to the contemporary Mueller Glacier and Mueller Lake. Mueller moraine height is ~120 m (photo source: author Carr, March 2018). (B) Location of Kea Point in relation to the Mueller Glacier and Mueller Lake in 1915 (photo source: du Faur, 1915). (C) Kea Point flood breach, viewed from Mueller Glacier moraine, at entrance to Hooker Glacier. Mueller Glacier has largely retreated out of sight, with only fragments of the terminus still visible (photo source: author Carr, March 2018). (D) Photograph of the original Hermitage Hotel following the 1913 flood (photo source: du Faur, 1915).

Figure 3 A schematic geomorphological map of the area surrounding the estimated path of the 1913 Kea Point outburst flood. Landforms were digitised from a satellite image (IKONOS-2; April 2003). Dates are determined from Schuster et al. (2009). Where applicable, a range of estimated moraine dates is provided.

Figure 4 (A) Orthoimage and (B) DEM produced using SfM photogrammetry of the study site. The walking track along the outburst channel is evident on (A) as a grey line. The position of cross-sections extracted to estimate peak discharge are shown. (C) to (F) Cross-sections and bankfull water levels. Background aerial imagery sourced from the LINZ Data Service and licensed for re-use under the Creative Commons Attribution 4.0 New Zealand licence.

Figure 5. Location maps highlighting (a) measured exposed position identifying the channel, moraine and braid data sets, (b) clast orientation relative to South, (c) clast roundness, according to Power's Roundness Index, and (d-f) clast A- B- and C-axis geometry, respectively.

Figure 6. Mueller Glacier showing Kea Point, pathway of outburst flood, and old and new Hermitage buildings as seen from Sebastopol. Photograph taken in 1915. Photo source: Hocken Collections, Uare Taoka o Hākena, University of Otago, <http://hockensnapshop.ac.nz/nodes/index/page:2/q:EBNH/j:3259>.

Figure 7. Timeline of triggers and events for the January (upper panel) and March (lower panel) 1913 Kea Point floods, and associated geomorphological impacts. For each flood, we note the date (black), major phase of the event (blue), description of the event (green) and sources (yellow).

Figure 8. Graphical summary of the downstream, reach-scale variations in longitudinal gradient (a), clast geometry (b-d), the boulder-axis-based estimates of flow velocity and discharge (e), and histograms for the subsamples' associated roundness (f) and orientation (g). Moraine data are shown for comparison owing to the likely source of the sediments deposited by the flood events. Note, in (g), the orientation of the notional thalweg is indicated with an arrow, and the outer margin of the rose diagram denotes the maximum axis scale for the number of clasts in 15° bins. Box-whisker plots show 25-75th percentiles (box), median (red line), whiskers (limits of data distribution) and outlying data (as in red crosses)..

Figure 9. Illustration of the RA/C₁ measures for the subsampled flood channel reaches (a) and a Zingg diagram indicating clast shape categorised only by the three descriptive environments (b).

Table captions

Table 1 Sources used in historical archival analysis

Table 2 Empirical equations used to estimate peak discharge (Q_p , m^3s^{-1}) (selected from those compiled by Kershaw et al, 2005). Here, A = cross-sectional area, m^2 ; R_h = hydraulic radius, m ; s = slope; D = nominal diameter, m .

Table 3 Estimates of peak discharge (m^3s^{-1}) from empirical equations. Location of transects are shown in Figure 4.

Table 4 Aggregated summary data for all clast measurements made in and proximate to the Kea Point flood path. For clast dimensions and orientation, mean (and SD) are given, while modal roundness is shown, along with calculated RA and C_{40} measures. NB. Values rounded given measurement uncertainty.

Table 5 Framework for how different resources can be used to provide information to reconstruct different aspects of a past flood event. ✓ indicates that a resource is likely to provide information on a particular aspect of a flood's source, pathway or receptor. ✓✓ indicates that a resource is highly likely to provide information on a particular aspect of a flood's source, pathway or receptor.

References

- Agatova, A.R., Nepop, R.K. 2019. Pleistocene fluvial catastrophes in now arid NW areas of Mongolian Inland drainage basin. *Global and Planetary Change*, 175, 211-225.
<https://doi.org/10.1016/j.gloplacha.2019.02.009>.
- Allen, S.K., Schneider, D., Owens, I.F. 2009. First approaches towards modelling glacial hazards in the Mount Cook region of New Zealand's Southern Alps. *Natural Hazards and Earth Systems Science*. 9, 481-499. 10.5194/nhess-9-481-2009.
- Allen, S.K., Cox, S.C., Owens, I.F. 2011. Rock avalanches and other landslides in the central Southern Alps of New Zealand: a regional study considering possible climate change impacts. *Landslides*. 8, 33-48. DOI 10.1007/s10346-010-0222-z.
- Ashburton Guardian. 1913. Heavy rainfall at the Hermitage, Ashburton Guardian, Volume XXXIII, Issue 8521, 29th of March 1913, <https://paperspast.natlib.govt.nz/newspapers/AG19130329.2.19.6>.
- Bakker, M., Lane, S. N. 2017. Archival photogrammetric analysis of river–floodplain systems using Structure from Motion (SfM) methods. *Earth Surface Processes and Landforms*. 42, 1274-1286. DOI: 10.1002/esp.4085.
- Barrell, D.J.A., Andersen, P.G., Denton, G.H. 2011. Glacial geomorphology of the central South Island, New Zealand. *GNS Science*.
- Beniston M. 2003. Climatic Change in Mountain Regions: A Review of Possible Impacts. In Diaz, H.F. (Ed.) *Climate Variability and Change in High Elevation Regions: Past, Present & Future*. Advances in Global Change Research, 15. Springer, Dordrecht. https://doi.org/10.1007/978-94-015-1252-7_2.
- Benito, G., Lang, M., Barriendos, M., Llasat, M.C., Francés, F., Ouarda, T., Thorndycraft, V., Enzel, Y., Bardossy, A., Coeur, D., Bobée, B., 2004. Use of Systematic, Palaeoflood and Historical Data for the Improvement of Flood Risk Estimation. Review of Scientific Methods. *Nat Hazards*, 31(3), 623-643. 10.1023/B:NHAZ.0000024895.48463.eb.

Benn, D.I., Ballantyne, C.K. 1994. Reconstructing the transport history of glacial sediments: a new approach based on the co-variance of clast form indices. *Sedimentary Geology*. 91, 215-227. [https://doi.org/10.1016/0037-0738\(94\)90130-9](https://doi.org/10.1016/0037-0738(94)90130-9).

Benn, D.I., Bolch, T., Hands, K., Gulley, J., Luckman, A., Nicholson, L.I., Quincey, D., Thompson, S., Toumi, R., Wiseman, S., 2012. Response of debris-covered glaciers in the Mount Everest region to recent warming, and implications for outburst flood hazards. *Earth-Science Reviews*, 114, 156-174. <https://doi.org/10.1016/j.earscirev.2012.03.008>.

Benn, D.I., Iton, N.R., 2010. An Excel™ spreadsheet program for reconstructing the surface profile of former mountain glaciers and ice caps. *Computers and Geosciences*. 36, 605-610. <https://doi.org/10.1016/j.cageo.2009.09.016>.

Blair Jr, R.W. 1994. Moraine and valley wall collapse due to rapid deglaciation in Mount Cook National Park, New Zealand. *Mountain Research and Development*. 14, 347-358. DOI: 10.2307/3673731.

Brázdil, R., Kundzewicz, Z. W., Benito, G. 2006. Historical hydrology for studying flood risk in Europe. *Hydrological Sciences Journal*. 51, 733-764. <https://doi.org/10.1623/hysj.51.5.739>.

Brázdil, R., Chromá, K., Rezníček, L., Valasek, H., Dolák, L., Stachon, Z., Soukalová, E., Dobrovolný, P. 2014. The use of taxation records in assessing historical floods in South Moravia, Czech Republic. *Hydrology and Earth System Sciences*. 18, 3873–3889. DOI: 10.5194/hess-18-3873-2014.

Breien, H., De Blasio, F.V., Elverhøi, A., Høeg, K. 2008. Erosion and morphology of a debris flow caused by a glacial lake outburst flood, Western Norway. *Landslides*. 5, 271-280. <https://doi.org/10.1007/s10346-008-0118-3>.

Brouwer, T., Eilander, D., Van Loenen, A., Booij, M.J., Wijnberg, K.M., Verkade, J.S., Wagemaker, J., 2017. Probabilistic flood extent estimates from social media flood observations. *Natural Hazards and Earth Systems Science*. 17, 735-747. <https://doi.org/10.5194/nhess-17-735-2017>.

Brown T.G. 2011. Dating surfaces and sediments, in Gregory, K.J., Goudie, A.S. (Eds.) The SAGE handbook of geomorphology. SAGE, London, pp. 192-209.

Burrows, C. J. 1973. Studies on some glacial moraines in New Zealand—2: Ages of moraines of the Mueller, Hooker and Tasman Glaciers. *New Zealand Journal of Geology and Geophysics*. 16, 831-856. DOI: 10.1080/00288306.1973.10555228

Calhoun, N.C., Clague, J.J. 2018. Distinguishing between debris flows and hyperconcentrated flows: an example from the eastern Swiss Alps. *Earth Surface Processes and Landforms*. 43, 1280– 1294. <https://doi.org/10.1002/esp.4313>.

Carling, P.A. 1986. The Noon Hill flash floods; July 17th 1983. Hydrological and geomorphological aspects of a major formative event in an upland landscape. *Transactions of the Institute of British Geographers*. 11, 105-118. DOI: 10.2307/622074.

Carrivick, J.L., Smith, M.W. 2019. Fluvial and aquatic applications of Structure from Motion photogrammetry and unmanned aerial vehicle/drone technology. *Wiley Interdisciplinary Reviews: Water*. 6, e1328. <https://doi.org/10.1002/wat2.1328>.

Carrivick, J.L., James, W.H.M., Grimes, M., Sutherland, J.L., Lorrey, A.M., 2020. Ice thickness and volume changes across the Southern Alps, New Zealand, from the little ice age to present. *Scientific Reports*. 10, 13392. <https://doi.org/10.1038/s41598-020-70276-8>.

Carrivick, J.L., Tweed, F.S. 2016. A global assessment of the societal impacts of glacier outburst floods. *Global and Planetary Change*. 144, 1-16. <https://doi.org/10.1016/j.gloplacha.2016.07.001>.

Cenderelli, D.A., Wohl E.E. 1998. Sedimentology and Clast Orientation of Deposits Produced by Glacial-Lake Outburst Floods in the Mount Everest Region, Nepal. In: Kalvoda J., Rosenfeld C.L. (eds) *Geomorphological Hazards in High Mountain Areas*. The GeoJournal Library. 46. Springer, Dordrecht.

Cenderelli, D.A., Wohl, E.E. 2001. Peak discharge estimates of glacial-lake outburst floods and “normal” climatic floods in the Mount Everest region, Nepal. *Geomorphology*. 40, 57-90. [https://doi.org/10.1016/S0169-555X\(01\)00037-X](https://doi.org/10.1016/S0169-555X(01)00037-X).

Chinn, T., Fitzharris, B.B., Willsman, A., Salinger, M.J. 2012. Annual ice volume changes 1976–2008 for the New Zealand Southern Alps. *Global and Planetary Change*. 92, 105-118. <https://doi.org/10.1016/j.gloplacha.2012.04.002>.

Chinn T.J., Kargel J.S., Leonard G.J., Haritashya U.K., Pleasants M. (2014) New Zealand’s Glaciers. In Kargel J., Leonard G., Bishop M., Käab A., Raup B. (Eds) *Global Land Ice Measurements from Space*. Springer Praxis Books. Springer, Berlin, Heidelberg. https://doi.org/10.1007/978-3-540-79818-7_29

Clague, J.J., Evans, S.G. 2000. A review of catastrophic drainage of moraine-dammed lakes in British Columbia. *Quaternary Science Reviews*. 19, 1763-1783. [https://doi.org/10.1016/S0277-3791\(00\)00090-1](https://doi.org/10.1016/S0277-3791(00)00090-1).

Clague, J.J., Huggel, C., Korup, O., McGuire, B. 2012. Climate change and hazardous processes in high mountains. *Revista de la Asociación Geológica Argentina*. 69, 328-338, <https://doi.org/10.5167/uzh-77920>.

Cody, E., Draebing, D., McCall, S., Cook, S., Brideau, M-A. 2020. Geomorphology and geological controls of an active paraglacial rockslide in the New Zealand Southern Alps. *Landslides*. 17, 755-776. <https://doi.org/10.1007/s10346-019-01316-2>.

Costa, J.E. 1983. Paleohydraulic reconstruction of flash-flood peaks from boulder deposits in the Colorado Front Range. *Geological Society of America Bulletin*. 94, 986-1004. [https://doi.org/10.1130/0016-7606\(1983\)94<986:PROFPP>2.0.CO;2](https://doi.org/10.1130/0016-7606(1983)94<986:PROFPP>2.0.CO;2).

Chinn, T.J.H. 1996. New Zealand glacier responses to climate change of the past century. *New Zealand Journal of Geology and Geophysics*. 39, 415-428. DOI: 10.1080/00288306.1996.9514723.

Cox, S.C., Allen, S.K. 2009. Vampire rock avalanches of January 2008 and 2003, Southern Alps, New Zealand. *Landslides*. 6, 161-166. DOI: 10.1007/s10346-009-0149-4.

Cutter, S.L., Ismail-Zadeh, A., Alcántara-Ayala, I., Altan, O., Baker, D.N., Briceño, S., Gupta, H., Holloway, A., Johnston, D., McBean, G.A. 2015. Global risks: Pool knowledge to stem losses from disasters. *Nature*. 522, 277-279. DOI: 10.1038/522277a.

de Bruijn, J.A., de Moel, H., Jongman, B., de Ruiter, M.C., Wagemaker, J., Aerts, J.C. 2019. A global database of historic and real-time flood events based on social media. *Scientific Data*. 6, 1-12. <https://doi.org/10.1038/s41597-019-0326-9>.

Department of Conservation (DOC). 2019. Visitors to Aoraki Mt Cook exceed 1 million. Office of the Minister of Conservation Media Release, 16 May 2019. <https://www.doc.govt.nz/news/media-releases/2019/visitors-to-aorakimt-cook-exceed-1-million/>

du Faur, F, 1915. *The Conquest of Mount Cook and other climbs : an account of four seasons' mountaineering on the Southern Alps of New Zealand*, George Allen and Unwin, London.

Eltner, A., Sofia, G. 2020. Chapter 1 Structure from motion photogrammetric technique. In Tarolli, P., Mudd, S.M. (Eds.), *Remote Sensing of Geomorphology*. 23, 1–24. Elsevier. <https://doi.org/https://doi.org/10.1016/B978-0-444-64177-9.00001-1>

Ely, L.L., Webb, R.H., Enzel, Y. 1992. Accuracy of post-bomb ^{137}Cs and ^{14}C in dating fluvial deposits. *Quaternary Research*. 38, 196-204. [https://doi.org/10.1016/0033-5894\(92\)90056-O](https://doi.org/10.1016/0033-5894(92)90056-O).

Evening Post. 1913. Rain generally, Evening Post, Volume LXXXV, Issue 73, 28th of March 1913, <https://paperspast.natlib.govt.nz/newspapers/EP19130328.2.96>

Feather J. 2003. The National Libraries of the United Kingdom. *Alexandria*. 15, 175-181. <https://doi.org/10.1177/095574900301500305>.

Fitzharris, B.B., Hay, J.E., Jones, P.D. 1992. Behaviour of New Zealand glaciers and atmospheric circulation changes over the past 130 years. *Holocene*. 2, 97–106. <https://doi.org/10.1177/095968369200200201>.

Fitzpatrick, F.A., Knox, J.C., Whitman, H.E. 1999. Effects of historical land-cover changes on flooding and sedimentation, North Fish Creek, Wisconsin (Vol. 99, No. 4083). US Department of the Interior, US Geological Survey.

Fondren, E., McCune, M.M. 2018. Archiving and Preserving Social Media at the Library of Congress: Institutional and Cultural Challenges to Build a Twitter Archive. *Preservation, Digital Technology & Culture*. 47, 33-44. <https://doi.org/10.1515/pdtc-2018-0011>

Foulds, S.A., Griffiths, H.M., Macklin, M.G., Brewer, P.A. 2014. Geomorphological records of extreme floods and their relationship to decadal-scale climate change. *Geomorphology*, 216, 193-207. <https://doi.org/10.1016/j.geomorph.2014.04.003>.

Frey, H., Haeberli, W., Linsbauer, A., Huguenot, C., Paul, F. 2010. A multi-level strategy for anticipating future glacier lake formation and associated hazard potentials. *Natural Hazards and Earth System Sciences*. 10, 339-352. <https://doi.org/10.5167/uzh-33174>.

Gellatly, A.F. 1982. Lichenometry as a relative-age dating method in Mount Cook National Park, New Zealand. *New Zealand Journal of Botany*. 20, 343-353. <https://doi.org/10.1080/0028825X.1982.10428503>.

Gellatly, A.F., 1984. The use of rock weathering-rind thickness to redetermine moraines in Mount Cook National Park, New Zealand. *Arctic and Alpine Research*. 16, 225-232. DOI: 10.1080/00040851.1984.12004409.

Gellatly, A.F., Chinn, T.J., Röthlisberger, F., 1988. Holocene glacier variations in New Zealand: a review. *Quaternary Science Reviews*. 7, 227-242. [https://doi.org/10.1016/0277-3791\(88\)90008-X](https://doi.org/10.1016/0277-3791(88)90008-X).

Glasser, N. F., Jansson, K., Mitchell, W. A., Harrison, S. 2006. The geomorphology and sedimentology of the 'Témpanos' moraine at Laguna San Rafael, Chile. *Journal of Quaternary Science*. 21, 629-643. DOI: 10.1002/jqs.1002.

Grabowski, R.C., Gurnell, A.M. 2016. Using historical data in fluvial geomorphology. In Kondolf, G.M., Piégay, H., (Eds.) *Tools in Fluvial Geomorphology*, Wiley, pp.56-76.

Griffiths, H.M., Tooth, S. 2020. Remembering and forgetting floods and droughts: lessons from the Welsh colony in Patagonia. *Cultural Geographies*. <https://doi.org/10.1177/1474474020963135>.

Griffiths, H. M., Salisbury, T. E. 2013. 'The tears I shed were Noah's flood': medieval genre, floods and the fluvial landscape in the poetry of Guto'r Glyn. *Journal of Historical Geography*, 40, 94-104. <https://doi.org/10.1016/j.jhg.2012.11.008>.

Griffiths, H.M., Salisbury, T.E., Tooth, S. 2017. 'May God place a bridge over the River Tywi' interrogating flood perceptions and memories in Welsh medieval poetry. In Endfield, G., Veale, L. (Eds.) *Cultural Histories, Memories and Extreme Weather: A Historical Geography Perspective* (Routledge Research in Historical Geography), Routledge, pp. 93-111.

Harrison, S., Kargel, J.S., Huggel, C., Reynolds, J., Shugar, D.H., Betts, R.A., Emmer, A., Glasser, N., Haritashya, U.K., Klimeš, J., Peirard, L. 2018. Climate change and the global pattern of moraine-dammed glacial lake outburst floods. *The Cryosphere*. 12, 1195-1209. <https://doi.org/10.5194/tc-12-1195-2018>.

Haeberli, W., Schaub, Y., Huggel, C. 2017. Increasing risks related to landslides from degrading permafrost into new lakes in de-glaciating mountain ranges. *Geomorphology*. 293, 405-417. <https://doi.org/10.1016/j.geomorph.2016.02.009>.

Hales, T.C., Roering, J.J. 2005. Climate-controlled variations in scree production, Southern Alps, New Zealand. *Geology*. 33, 701-704. 10.1130/g21528.1.

- Harrison, S., Glasser, N., Winchester, V., Haresign, E., Warren, C., Jansson, K. 2006. A glacial lake outburst flood associated with recent mountain glacier retreat, Patagonian Andes. *The Holocene*. 16, 611-620. <https://doi.org/10.1191/0959683606hl957rr>
- Hawera and Normanby Star. 1913. Mount Cook, Hawera and Normanby Star, Volume XVIII, Issue XVIII, 21st of January 1913 <https://paperspast.natlib.govt.nz/newspapers/HNS19130121.2.27>
- Henderson, R. D., Thompson S. M. 1999. Extreme rainfalls in the Southern Alps of New Zealand, *Journal of Hydrology (New Zealand)*. 38, 309-330.
- Himmelsbach, I., Glaser, R., Schoenbein, J., Riemann, D., Martin B. . 2015. Reconstruction of flood events based on documentary data and transnational flood risk analysis of the Upper Rhine and its French and German tributaries since AD 1480. *Hydrology and Earth System Sciences*, 19, 4149–4164. <https://doi.org/10.5194/hess-19-4149-2015>.
- Hock, R., G. Rasul, C. Adler, B. Cáceres, S. Crüner, Y. Hirabayashi, M. Jackson, A. Kääb, S. Kang, S. Kutuzov, A. Milner, U. Molau, S. Morin, B. Orlove, and H. Steltzer. 2019. High Mountain Areas. In: H.-O. Pörtner, D.C. Roberts, V. Masson-Delmotte, P. Zhai, M. Tignor, E. Poloczanska, K. Mintenbeck, A. Alegría, M. Nicolai, A. Okem, J. Petzold, B. Rama, N.M. Weyer (eds.) *IPCC Special Report on the Ocean and Cryosphere in a Changing Climate*. <https://www.ipcc.ch/srocc/chapter/chapter-2/>
- Hoelzle, M., Chinn, T., Stunnenberg, D., Paul, F., Zemp, M., Haeberli, W. 2007. The application of glacier inventory data for estimating past climate change effects on mountain glaciers: a comparison between the European Alps and the Southern Alps of New Zealand. *Global and Planetary Change*. 56, 69-82. <https://doi.org/10.1016/j.gloplacha.2006.07.001>.
- Holdgate, M. W. 1979. A perspective of environmental pollution. Cambridge University Press Cambridge.

- Høgaas, F., Longva, O. 2016. Mega deposits and erosive features related to the glacial lake Nedre Glomsjø outburst flood, southeastern Norway. *Quaternary Science Reviews*. 151, 273-291. <https://doi.org/10.1016/j.quascirev.2016.09.015>.
- Hooke, J.J.M., Kain, R.R.J. 1982. Historical change in the physical environment: a guide to sources and techniques. Butterworth-Heinemann.
- Hutton, F. W. 1888. Notes on the Mueller glacier, New Zealand. *Proceedings of the Linnaean Society of New South Wales*. (2nd Series). 3, 429-42.
- Hyndman, D., Hyndman, D. 2016. Natural hazards and disasters. Cengage Learning.
- Iseli, J. G. 1991. Ice avalanche activity in Mount Cook National Park, unpublished M.Sc. thesis, Department of Geography, University of Canterbury, Christchurch, 151pp.
- IPCC. 2019. IPCC Special Report on the Ocean and Cryosphere in a Changing Climate, 765 pp.
- Jacquet, J., McCoy, S.W., Mcgrath, D., Nimick, D.A., Fahey, M., O'kuinghttons, J., Friesen, B.A., Leidich, J. 2017. Hydrologic and geomorphic changes resulting from episodic glacial lake outburst floods: Rio Colonia, Patagonia, Chile. *Geophysical Research Letters*. 44, 854-864. <https://doi.org/10.1002/2016GL071374>.
- Jeffers, J.M., 2014. Environmental knowledge and human experience: using a historical analysis of flooding in Ireland to challenge contemporary risk narratives and develop creative policy alternatives. *Environmental Hazards*. 13, 229-247. <https://doi.org/10.1080/17477891.2014.902800>.
- Jones, A.F., Macklin, M.G., Brewer, P.A. 2012. A geochemical record of flooding on the upper River Severn, UK, during the last 3750 years. *Geomorphology*. 179, 89-105. <https://doi.org/10.1016/j.geomorph.2012.08.003>.

- Kemp, J., Olley, J.M., Ellison, T., McMahon, J. 2015. River response to European settlement in the subtropical Brisbane River, Australia. *Anthropocene*, 11, 48-60. <https://doi.org/10.1016/j.ancene.2015.11.006>.
- Kerr, T., Owens, I., Henderson, R. 2011. The precipitation distribution in the Lake Pukaki Catchment. *Journal of Hydrology (New Zealand)*, 50, 361-382. www.jstor.org/stable/43945031.
- Kershaw, J.A., Clague, J.J., Evans, S.G. 2005. Geomorphic and sedimentological signature of a two-phase outburst flood from moraine-dammed Queen Bess Lake, British Columbia, Canada. *Earth Surface Processes and Landforms*. 30, 1-25. <https://doi.org/10.1002/esp.1122>.
- Kirkbride, M.P. 1993. The temporal significance of transitions from melting to calving termini at glaciers in the central Southern Alps of New Zealand. *The Holocene*. 3, 232-240. <https://doi.org/10.1177/095968369300300305>.
- Kirkbride, M.P., Winkler, S., 2012. Correlation of Late Quaternary moraines: impact of climate variability, glacier response, and chronological resolution. *Quaternary Science Reviews*. 46, 1-29. <https://doi.org/10.1016/j.quascirev.2012.04.002>.
- Kougkoulos, I., Cook, S.J., Edwards, L.A., Clarke, L.J., Symeonakis, E., Dortch, J.M., Nesbitt, K., 2018. Modelling glacial lake outburst flood impacts in the Bolivian Andes. *Natural Hazards*. 94, 1415-1438. <https://doi.org/10.1007/s11069-018-3486-6>.
- Lave, R., Wilson, M.W., Barron, E.S., Biermann, C., Carey, M.A., Duvall, C.S., Johnson, L., Lane, K.M., McClintock, N., Munroe, D., Pain, R. 2014. Intervention: Critical physical geography. *The Canadian Geographer/Le Géographe canadien*. 58, 1-10. <https://doi.org/10.1111/cag.12061>.
- Li, H., Ng, F., Li, Z., Qin, D., Cheng, G. 2012. An extended “perfect-plasticity” method for estimating ice thickness along the flow line of mountain glaciers. *Journal of Geophysical Research: Earth Surface*, 117. <https://doi.org/10.1029/2011JF002104>.

- Lorrey, A., Fauchereau, N., Stanton, C., Chappell, P., Phipps, S., Mackintosh, A., Renwick, J., Goodwin, I. & Fowler, A. 2014. The Little Ice Age climate of New Zealand reconstructed from Southern Alps cirque glaciers: a synoptic type approach. *Climate Dynamics*, 42, 3039-3060. <https://doi.org/10.1007/s00382-013-1876-8>
- Lumbroso, D., Gaume, E. 2012. Reducing the uncertainty in indirect estimates of extreme flash flood discharges. *Journal of Hydrology*. 414-415, 16-30. <https://doi.org/10.1016/j.jhydrol.2011.08.048>.
- Lyttelton Times. 1913. Heavy rains at Mount Cook, Lyttelton Times, Volume CXIV, Issue 16145, 23rd of January 1913 https://paperspast.natlib.govt.nz/newspapers/LT_1913_1123.2.88.
- Macklin, M.G., Fuller, I.C., Jones, A.F., Bebbington, M. 2012. New Zealand and UK Holocene flooding demonstrates interhemispheric climate synchrony. *Geology*. 40, 775-778. <https://doi.org/10.1130/g33364.1>.
- Marriott S. 1992. Textural analysis and modelling of a flood deposit: River Severn, U.K. *Earth Surface Processes and Landforms*. 17, 687-697. <https://doi.org/10.1002/esp.3290170705>.
- Marshall P. 1907. Notes on glaciation in New Zealand. Report of the Australasian Association for the Advancement of Science. 11, 283-289.
- Marston, R.A. 2008. Land, life, and environmental change in mountains. *Annals of the Association of American Geographers*. 98, 507-520. <https://doi.org/10.1080/00045600802118491>.
- McColl, S.T. 2012. Paraglacial rock-slope stability. *Geomorphology*. 153, 1-16. <https://doi.org/10.1016/j.geomorph.2012.02.015>.
- McDowell, G., Stephenson, E., Ford, J. 2014. Adaptation to climate change in glaciated mountain regions. *Climatic Change*. 126, 77-91. <https://doi.org/10.1007/s10584-014-1215-z>.

Mosley, P., Pearson, C. 1997. Introduction: hydrological extremes and climate in New Zealand. In Mosley, M.P., Pearson, C.P. (Eds.), *Floods and Droughts: the New Zealand Experience*, New Zealand Hydrological Society, Wellington North, New Zealand, pp. 1-14.

Nie, Y., Liu, Q., Wang, J., Zhang, Y., Sheng, Y., Liu, S. 2018. An inventory of historical glacial lake outburst floods in the Himalayas based on remote sensing observations and geomorphological analysis. *Geomorphology*. 308, 91-106. <https://doi.org/10.1016/j.geomorph.2018.02.002>.

Oamaru Mail. 1913. The Hermitage Flood, Oamaru Mail, Volume X: XVIII, Issue 11903, 12th of April 1913 <https://paperspast.natlib.govt.nz/newspapers/OAM19130412.2.29>.

Papers Past. 2020. <https://paperspast.natlib.govt.nz> (accessed 15th June, 2020).

Pellitero, R., Rea, B.R., Spagnolo, M., Bakke, J., Ivy-Ochs, S., Hew, C.R., Hughes, P., Ribolini, A., Lukas, S., Renssen, H. 2016. GlaRe, a GIS tool to reconstruct the 3D surface of palaeoglaciers. *Computers & Geosciences*. 94, 77-85. <https://doi.org/10.1016/j.cageo.2016.06.008>.

Pelto, M. 2018. Mueller Glacier, NZ Terminus Collapse, <https://blogs.agu.org/fromaglaciersonperspective/2018/02/23/mueller-glacier-nz-terminus-collapse/>
Accessed 14th August 2020.

Pierson, T.C. 2005. Hyperconcentrated flow—transitional process between water flow and debris flow. In Jakob, M., Hungr, O. (eds) *Debris-flow hazards and related phenomena*. Springer, Berlin Heidelberg, pp 159–202.

Poverty Bay Herald. 1913a. Last nights' telegrams, Poverty Bay Herald, Vol. XXXX (12961), 21st of January, 1913 <https://paperspast.natlib.govt.nz/newspapers/PBH19130121.2.13>.

Poverty Bay Herald. 1913b. Flood at the Hermitage, Poverty Bay Herald, Volume XXXX, Issue 12963, 23rd of January 1913, <https://paperspast.natlib.govt.nz/newspapers/PBH19130123.2.3>.

Poverty Bay Herald. 1913c. An awesome sight, Poverty Bay Herald, Volume XXXX, Issue 13024, 7th of April 1913 <https://paperspast.natlib.govt.nz/newspapers/PBH19130407.2.79.1>.

Press. 1913a. Floods at the Hermitage, Press, Volume XLIX, Issue 14626, 29th of March 1913, <https://paperspast.natlib.govt.nz/newspapers/CHP19130329.2.83.1>.

Press. 1913b. The floods at the Hermitage, Press, Volume XLIX, Issue 14631, 4th of April 1913 <https://paperspast.natlib.govt.nz/newspapers/CHP19130404.2.22.1>.

Reznichenko, N.V., Davies, T.R., Winkler, S. 2016. Revised palaeoclimatic significance of Mueller Glacier moraines, Southern Alps, New Zealand. *Earth Surface Processes and Landforms*. 41, 196-207. <https://doi.org/10.1002/esp.3848>.

Richardson, S.D. Reynolds, J.M. 2000. Degradation of ice-cored moraine dams: implications for hazard development. *IAHS PUBLICATION*, pp.187-197.

Riggs, H. 1976. A simplified slope-area method for estimating flood discharges in natural channels. *Journal of Research of the US Geological Survey*. 4, 285-291.

Robertson, C.M., Benn, D.I., Brook, M.S., Holt, K.A. 2012. Subaqueous calving margin morphology at Mueller, Hooker and Tasman glaciers in Aoraki/Mount Cook National Park, New Zealand. *Journal of Glaciology*. 58, 1037-1046. <https://doi.org/10.3189/2012JoG12J048>.

Röhl, K. 2008. Characteristics and evolution of supraglacial ponds on debris-covered Tasman Glacier, New Zealand. *Journal of Glaciology*. 54, 867-880. <https://doi.org/10.3189/002214308787779861>.

Ross, M. 1893. Aorangi; or the heart of the Southern Alps, New Zealand. Government Printer, Wellington.

Rosser, J.F., Leibovici, D.G, Jackson, M.J. 2017. Rapid flood inundation mapping using social media, remote sensing and topographic data. *Natural Hazards*, 87, 103-120. <http://doi.org/10.1007/s11069-017-2755-0>

Rounce, D.R., McKinney, D.C., Lala, J.M., Byers, A.C., Watson, C.S. 2016. A new remote hazard and risk assessment framework for glacial lakes in the Nepal Himalaya. *Hydrology and Earth System Sciences*. 20, 3455-3475. <http://doi.org/10.5194/hess-20-3455-2016>.

Schaefer, J.M., Denton, G.H., Kaplan, M., Putnam, A., Finkel, R.C., Barrell, D.J.A., Andersen, B.G., Schwartz, R., Mackintosh, A., Chinn, T., Schlüchter, C. 2009. High-frequency Holocene glacier fluctuations in New Zealand differ from the northern signature. *Science*. 324. 622–625. DOI:10.1126/science.1169312

Schulte, L., Peña, J.C., Carvalho, F., Schmidt, T., Julià, R., Llorca, J., Veit, H. 2015. A 2600-year history of floods in the Bernese Alps, Switzerland: frequencies, mechanisms and climate forcing. *Hydrol. Earth Syst. Sci.* 19(7), 3047-3072. <http://doi.org/10.5194/hess-19-3047-2015>.

Schulte, L., Wetter, O., Wilhelm, B., Peña, J.C., Amann, P., Wirth, S.B., Carvalho, F., Gómez-Bolea, A. 2019a. Integration of multi-archive datasets for the development of a four-dimensional paleoflood model of alpine catchments. *Global and Planetary Change*. 180, 66-88. <https://doi.org/10.1016/j.gloplacha.2019.05.011>.

Schulte, L., Schillereff, D., Santisteban, J.I., 2019b. Pluridisciplinary analysis and multi-archive reconstruction of paleofloods: Societal demand, challenges and progress. *Global and Planetary Change*. 177. 225-238. <http://doi.org/10.1016/j.gloplacha.2019.03.019>

Schulte, L., Schillereff, D., Santisteban, J.I., Marret-Davies, F., 2020. Pluridisciplinary analysis and multi-archive reconstruction of paleofloods. *Global and Planetary Change*. 191. 103220. <http://doi.org/10.1016/j.gloplacha.2020.103220>.

Shugar, D.H., Burr, A., Haritashya, U.K., Kargel, J.S., Watson, C.S., Kennedy, M.C., Bevington, A.R., Betts, R.A., Harrison, S., Strattman, K., 2020. Rapid worldwide growth of glacial lakes since 1990. *Nature Climate Change*, 10, 939-945. <https://doi.org/10.1038/s41558-020-0855-4>

Slaymaker, O. 2010. Mountain hazards. In Alcántara-Ayala I., Goudie, A. (Eds) Geomorphological hazards and disaster prevention. Cambridge University Press, Cambridge, 33-48.

Staines, K.E., Carrivick, J.L. 2015. Geomorphological impact and morphodynamic effects on flow conveyance of the 1999 jökulhlaup at sólheimajökull, Iceland. *Earth Surface Processes and Landforms*. 40, 1401-1416. <https://doi.org/10.1002/esp.3750>.

Star. 1913a. Disastrous storm, Star, Issue 10729, 29th of March 1913, <https://paperspast.natlib.govt.nz/newspapers/TS19130329.2.64>.

Star. 1913b. Disastrous storm, Star, Issue 10730, 31st of March 1913, <https://paperspast.natlib.govt.nz/newspapers/TS19130331.2.66>.

Stott, E., Williams, R.D., Hoey, T.B. 2020. Ground Control Point Distribution for Accurate Kilometre-Scale Topographic Mapping Using an RTK-GNSS Unmanned Aerial Vehicle and SfM Photogrammetry. *Drones*, 4, 55. <https://doi.org/10.3390/drones4030055>.

Taylor, F.E., Malamud, B.D., Freeborough, V., Demeritt, D. 2015. Enriching Great Britain's National Landslide Database by searching newspaper archives. *Geomorphology*. 249, 52-68. <https://doi.org/10.1016/j.geomorph.2015.05.019>.

Teng, J., Jakeman, A.J., Vaze, J., Croke, B.F., Dutta, D., Kim, S. 2017. Flood inundation modelling: A review of methods, recent advances and uncertainty analysis. *Environmental Modelling & Software*. 90, 201-216. <https://doi.org/10.1016/j.envsoft.2017.01.006>.

Timaru Herald. 1913a. The Hermitage Flood, Timaru Herald, Volume XCVII, Issue 14955, 24th of January, 1913 <https://paperspast.natlib.govt.nz/newspapers/THD19130124.2.18>.

Timaru Herald. 1913b. Heavy rain and floods at the Hermitage, Timaru Herald, Volume XCVII, Issue 14952, 21st of January 1913 <https://paperspast.natlib.govt.nz/newspapers/THD19130121.2.14>.

Timaru Herald. 1913c. The Hermitage Flood, Timaru Herald, Volume XCVII, Issue 14957, 27th of January 1913, <https://paperspast.natlib.govt.nz/newspapers/THD19130127.2.7>.

Timaru Herald. 1913d. Heavy rains, Timaru Herald, Volume XCVII, Issue 15007, 29 March 1913, <https://paperspast.natlib.govt.nz/newspapers/THD19130329.2.45>.

Timaru Herald. 1913e. Mount Cook cars, Timaru Herald, Volume XCVII, Issue 15011, 3rd of April 1913 <https://paperspast.natlib.govt.nz/newspapers/THD19130403.2.51>.

Timaru Herald. 1913f. The Hermitage Flood, Timaru Herald, Volume XCVII, Issue 14954, 23rd of January 1913 <https://paperspast.natlib.govt.nz/newspapers/THD19130123.2.17>.

Tourist And Health Resorts Department. 1913. Annual Report of the Tourist And Health Resorts Department, By The Minister Of Tourist And Health Resorts Hon. R. Heaton Rhodes., Appendix to the Journals of the House of Representatives, 1913 Session I, H-02, <https://paperspast.natlib.govt.nz/parliamentary/AJHR1913-I.2.5.2.2>.

Trimble, S.W. 2008. The use of historical data and artifacts in geomorphology. *Progress in Physical Geography*. 32, 3-29. <https://doi.org/10.1177/0309133308089495>.

Vautherin, J., Rutishauser, S., Schneider-Zapp, K., Choi, H.F., Chovancova, V., Glass, A., Strecha, C. 2016. Photogrammetric accuracy and modeling of rolling shutter cameras. *ISPRS Annals of Photogrammetry, Remote Sensing & Spatial Information Sciences*. 3, 139-146.

Veh, G., Korup, O., von Specht, S., Roessner, S., Walz, A., 2019. Unchanged frequency of moraine-dammed glacial lake outburst floods in the Himalaya. *Nature Climate Change*. 9, 379-383. <https://doi.org/10.1038/s41558-019-0437-5>.

Viviroli, D., Archer, D.R., Buytaert, W., Fowler, H.J., Greenwood, G.B., Hamlet, A.F., Huang, Y., Koboltschnig, G., Litaor, M.I., López-Moreno, J.I., Lorentz, S. 2011. Climate change and mountain water resources: overview and recommendations for research, management and policy. *Hydrology and Earth System Sciences*. 15, 471-504. <https://doi.org/10.5167/uzh-109709>.

- Vilímek, V., Klimeš, J., Emmer, A., Benešová, M. 2015. Geomorphologic impacts of the glacial lake outburst flood from Lake No. 513 (Peru). *Environmental Earth Sciences*. 73, 5233-5244. <https://doi.org/10.1007/s12665-014-3768-6>.
- Wang, R-Q., Mao, H., Wang, Y., Rae, C., Shaw, W. 2018. Hyper-resolution monitoring of urban flooding with social media and crowdsourcing data. *Computers & Geosciences*. 111, 139-147. <https://doi.org/10.1016/j.cageo.2017.11.008>.
- Wanganui Chronicle. 1913. Disastrous flood, Wanganui Chronicle, issue 12881, 31st of March 1913 <https://paperspast.natlib.govt.nz/newspapers/WC19130331.2.30.1.1>.
- Westoby, M.J., Glasser, N.F., Hambrey, M.J., Brasington, J., Reynolds, J.M., Hassan, M.A. 2014. Reconstructing historic Glacial Lake Outburst Floods through numerical modelling and geomorphological assessment: Extreme events in the Himalaya. *Earth Surface Processes and Landforms*. 39, 1675-1692. <https://doi.org/10.1002/esp.3617>.
- Westoby, M., Brasington, J., Glasser, N., Hambrey, M., Reynolds, J., Hassan, M., Lowe, A. 2015. Numerical modelling of glacial lake outburst floods using physically based dam-breach models. *Earth Surface Dynamics*. 3, 171-199. <http://dx.doi.org/10.5194/esurf-3-171-2015>.
- Wetter, O., Pfister, C., Weingartner, R., Luterbacher, J., Reist, T., Trösch, J. 2011. The largest floods in the high Rhine basin since 1268 assessed from documentary and instrumental evidence. *Hydrological Sciences Journal*. 56, 733–758. <https://doi.org/10.1080/02626667.2011.583613>.
- Whitehouse, I.E. 1982. Erosion on Sevastopol, Mt Cook, New Zealand, in the Last 85 Years. *New Zealand Geographer*. 38, 77-80. <https://doi.org/10.1111/j.1745-7939.1982.tb00996.x>.
- Whitehouse, I.E. 1988. Geomorphology of the central Southern Alps, New Zealand: the interaction of plate collision and atmospheric circulation. *Zeitschrift für Geomorphologie Supplementband*. 69, 105–116. <http://pascal-francis.inist.fr/vibad/index.php?action=getRecordDetail&idt=6797187>.

Wilhelm, B., Ballesteros Cánovas, J.A., Macdonald, N., Toonen, W.H., Baker, V., Barriendos, M., Benito, G., Brauer, A., Corella, J.P., Denniston, R., Glaser, R. 2019. Interpreting historical, botanical, and geological evidence to aid preparations for future floods. *Wiley Interdisciplinary Reviews: Water*. 6, p.e1318. <https://doi.org/10.1002/wat2.1318>.

Wilkinson, C., Hikuroa, D. C. H., Macfarlane, A. H., Hughes, M. W. 2020. Mātauranga Māori in geomorphology: existing frameworks, case studies, and recommendations for incorporating Indigenous knowledge in Earth science, *Earth Surface Dynamics*, 8, 595–618, <https://doi.org/10.5194/esurf-8-595-2020>, 2020.

Williams, G.P. 1978. Bank-full discharge of rivers. *Water resources research*. 14, 1141-1154. <https://doi.org/10.1029/WR014i006p01141>

Williams, G.P. 1983. Paleohydrological methods and some examples from Swedish fluvial environments: I cobble and boulder deposits. *Geografiska Annaler: Series A, Physical Geography*. 65, 227-243. <https://doi.org/10.1080/04353676.1983.11880088>.

Williams, R.D., Measures, R., Hicks, D.M., Frasington, J. 2016. Assessment of a numerical model to reproduce event-scale erosion and deposition distributions in a braided river. *Water Resources Research*, 52, 6621-6642. <https://doi.org/10.1002/2015WR018491>.

Wilson, R., Harrison, S., Reynolds, J., Hubbard, A., Glasser, N.F., Wünderlich, O., Iribarren Anaconda, P., Mao, L., Shannon, S., 2019. The 2015 Chileno Valley glacial lake outburst flood, Patagonia. *Geomorphology*, 332, 51-65. <https://doi.org/10.1016/j.geomorph.2019.01.015>.

Winkler, S. 2000. The 'Little Ice Age' maximum in the Southern Alps, New Zealand: preliminary results at Mueller Glacier. *The Holocene*. 10, 643– 647. <https://doi.org/10.1191/095968300666087656>.

Yan, X.H., Boyer, T., Trenberth, K., Karl, T.R., Xie, S.P., Nieves, V., Tung, K.K. Roemmich, D. 2016. The global warming hiatus: Slowdown or redistribution? *Earth's Future*, 4, 472-482. <https://doi.org/10.1002/2016EF000417>.

Zaginaev, V., Petrakov, D., Erokhin, S., Meleshko, A., Stoffel, M., Ballesteros-Cánovas, J.A. 2019. Geomorphic control on regional glacier lake outburst flood and debris flow activity over northern Tien Shan. *Global and Planetary Change*, 176, 50-59. <https://doi.org/10.1016/j.gloplacha.2019.03.003>.

Table 1 Sources used in historical archival analysis

Type of source	Specific sources used	Information on 20 January 1913 event	Information on 28 March 1913 event	Reference
Newspaper article	Ashburton Guardian		✓	Ashburton Guardian (1913)
	Evening Post		✓	Evening Post (1913)
	Hawera and Normanby Star	✓		Hawera and Normanby Star (1913)
	Lyttelton Times	✓		Lyttelton Times (1913)
	Oamaru Mail		✓	Oamaru Mail (1913)
	Poverty Bay Herald	✓	✓	Poverty Bay Herald (1913a,b,c)
	Press		✓	Press (1913a,b)
	Star		✓	Star (1913a, b)
	Timaru Herald	✓	✓	Timaru Herald (1913a,b,c,d,e,f)
	Wanganui Chronicle		✓	Wanganui Chronicle (1913)
Diary/ Travelogue	The Conquest of Mount Cook and other climbs: an account of four seasons' mountaineering on the Southern Alps of New Zealand	✓	✓	du Faur, (1915)
Parliamentary paper	Annual Report of the Tourist And Health Resorts Department	✓	✓	Tourist And Health Resorts Department (1913)

Table 2 Empirical equations used to estimate peak discharge (Q_p , m^3s^{-1}) (selected from those compiled by Kershaw et al, 2005). Here, A = cross-sectional area, m^2 ; R_h = hydraulic radius, m ; s = slope; D = nominal diameter, m .

Approach	Method	Equation
Slope-area	Manning equation	$Q_p = AR_h^{2/3} s^{1/2}$
	Riggs (1976)	$Q_p = 3.39 A^{1.30} s^{0.32}$
	Williams (1978)	$Q_p = 4.0 A^{1.21} s^{0.28}$
Boulder measurements	Costa (1983)	$Q_p = 493.691 D^{1.908}$

Table 3 Estimates of peak discharge (m^3s^{-1}) from empirical equations. Location of transects are shown in Figure 4.

Transect	Slope-Area approach			Boulder measurement approach		
	Manning equation	Riggs (1976)	Williams (1978)	Costa (1983)	Min.	Max.
						Mean and standard deviation
1	522	998	827		204	2419
2	316	629	538		362	4093*
3	361	771	654		211	1818
4	430	1077	906		256	2459

*Excluding an outlier with a b-axis of 4.97 m and $Q = 10522 m^3s^{-1}$.

Table 4 Aggregated summary data for all clast measurements made in and proximate to the Kea Point flood path. For clast dimensions and orientation, mean (and SD) are given, while modal roundness is shown, along with calculated RA and C_{40} measures. NB. Values rounded given measurement uncertainty.

Metric	Aggregated	Channel	Braid	Moraine
n	843	706	77	60
A-axis (mm)	1380 (860)	1410 (870)	750 (310)	1890 (820)
B-axis (mm)	900 (590)	920 (600)	500 (210)	1200 (550)
C-axis (mm)	560 (370)	567 (380)	350 (160)	730 (360)
Roundness	SA	SA	SA	SR
Orientation (°)	-1 (50)	0 (50)	-4 (45)	-5 (51)
RA (%)	26	28	12	8
C_{40} (%)	48	49	38	52

Table 5 Framework for how different resources can be used to provide information to reconstruct different aspects of a past flood event. ✓ indicates that a resource is likely to provide information on a particular aspect of a flood's source, pathway or receptor. ✓✓ indicates that a resource is highly likely to provide information on a particular aspect of a flood's source, pathway or receptor.

Resource	Source				Pathway			Receptor			Application
	Event date	Rainfall temporal dynamics	Rainfall quantity	Rainfall spatial distribution	Spatial flood extent	Flood routing timing	Discharge quantity	Geomorphic change	Property damage	Injury / fatality	
Historical documents	✓✓	✓	✓		✓	✓	✓	✓	✓✓	✓✓	Used in this investigation
Sedimentological					✓		✓				
Geomorphological					✓		✓	✓			
Stratigraphic / biostratigraphic dating	✓										Potential for other investigations
Environmental monitoring network*	✓✓	✓✓	✓✓	✓	✓	✓	✓				
Numerical modelling					✓✓	✓✓	✓✓	✓	✓		
Satellite remote sensing	✓	✓	✓	✓	✓	✓	✓	✓	✓		
Interviews	✓	✓			✓	✓		✓	✓	✓	

* i.e. rainfall and discharge gauges

Abstract

Flood reconstruction is essential for establishing magnitude-frequency relationships and assessments of contemporary geohazards and risks. Traditionally, flood reconstructions rely upon the analysis of evidence acquired from a single discipline. This lack of integration limits the insights into a flood's source, pathway, and receptors (i.e. impacts). Here, our aim is to test the integration of qualitative historical documentary material with quantitative geomorphological and sedimentological evidence to reconstruct glacial lake outburst floods (GLOFs) in 1913 at Kea Point, Mount Cook National Park, Aotearoa New Zealand. Written documentary records show that, following heavy rainfall, GLOF events occurred in January and March, after the temporary impoundment of water between the glacier surface and lateral moraine. Peak flood discharge was estimated from slope-area and exposed boulder measurements as $316\text{-}1077\text{ m}^3\text{s}^{-1}$ and $496\text{-}1622\text{ m}^3\text{s}^{-1}$ respectively. Sedimentological information, combined with geomorphic mapping, a DEM derived from Structure from Motion (SfM) photogrammetry, and satellite imagery was used to describe the overall physical impact of the GLOF. Information from written documentary records, however, enabled a more detailed reconstruction of the timeline of the two floods and their impacts proximate to the original 'Hermitage Hotel', which was subsequently relocated. Our integrated approach exemplifies the informative level of multi-faceted detail that can be retrieved for historical flood events. We propose a framework for future studies that seek to reconstruct flood events and their source, pathway and receptors through combining evidence from historical documents/artefacts, sedimentological/geomorphological data, and integration with environmental monitoring/modelling outputs.

Declaration of Competing Interest

On behalf of myself and the co-authors of the above manuscript, I declare no competing interests associated with the manuscript.

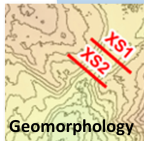
Journal Pre-proof



Sedimentology






Written
documentary
records



Geomorphology

INTEGRATED RECONSTRUCTION OF 1913 KEA POINT FLOODS

GENERIC RECONSTRUCTION FRAMEWORK

	Source 	Pathway 	Receptor 
Historical documents	✓	✓	✓
Sedimentological		✓	
Geomorphological		✓	✓
Dating	✓		
Gauge network	✓	✓	
Numerical modelling		✓	✓
Interviews	✓	✓	✓
Satellite remote sensing	✓	✓	✓

Graphics Abstract

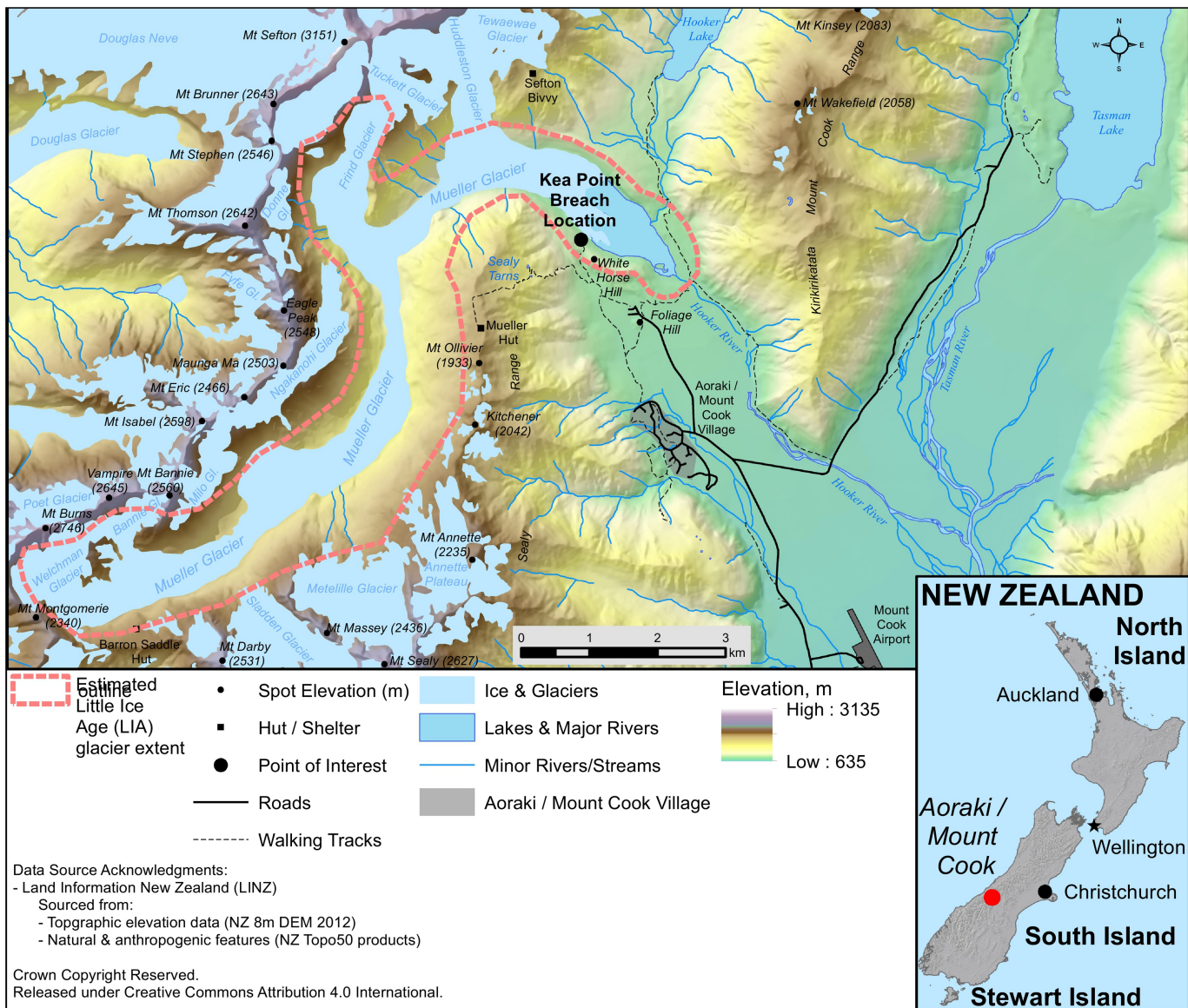


Figure 1

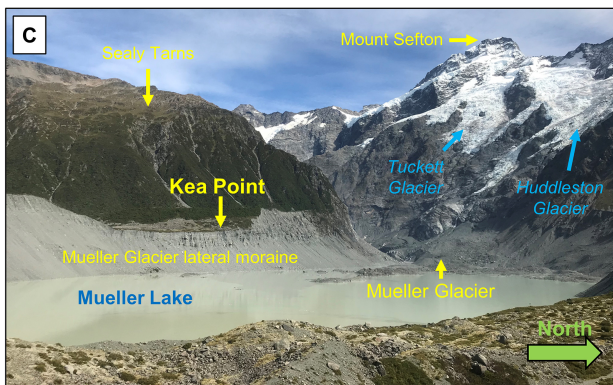
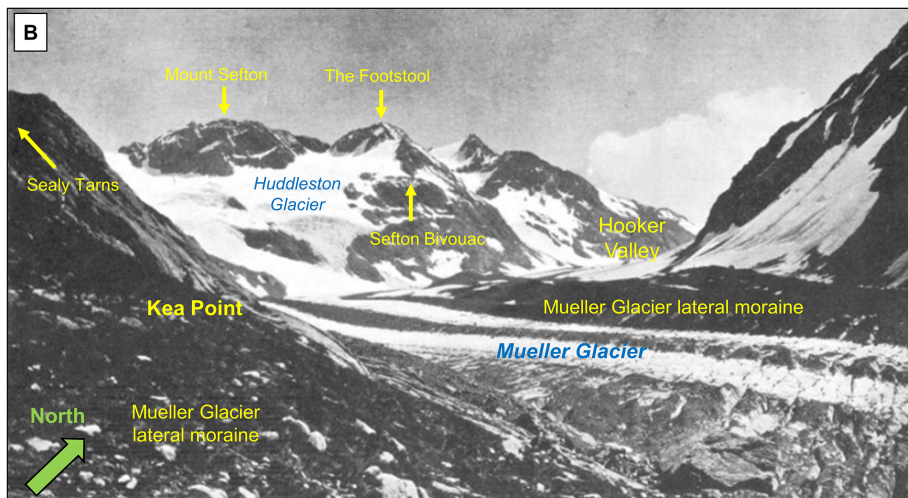
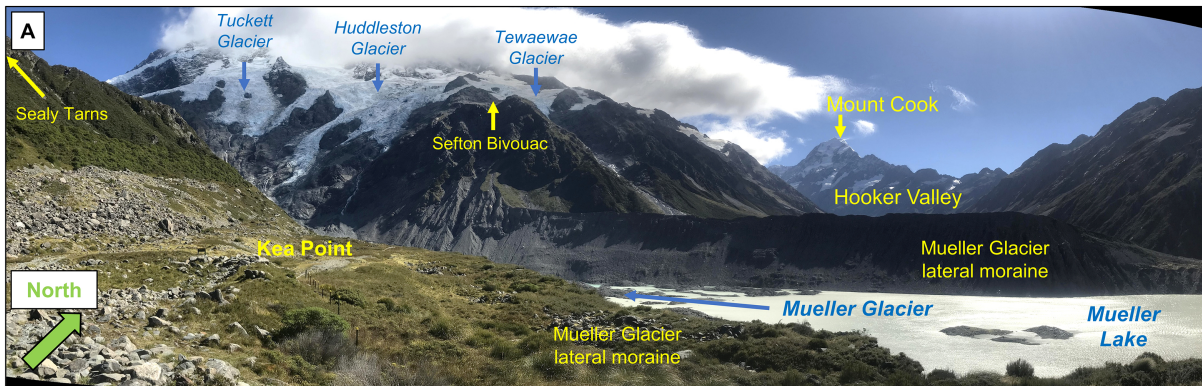


Figure 2

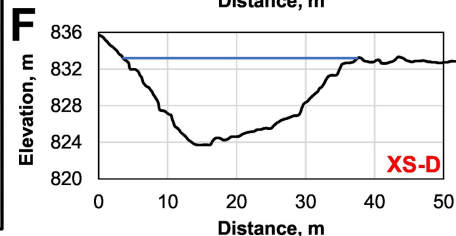
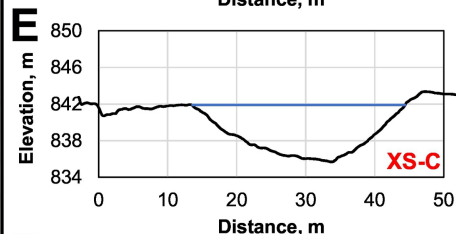
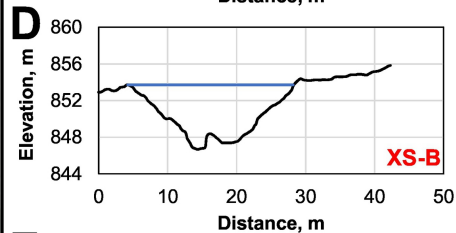
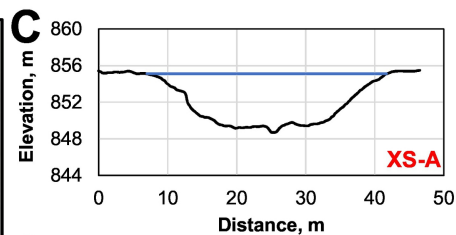
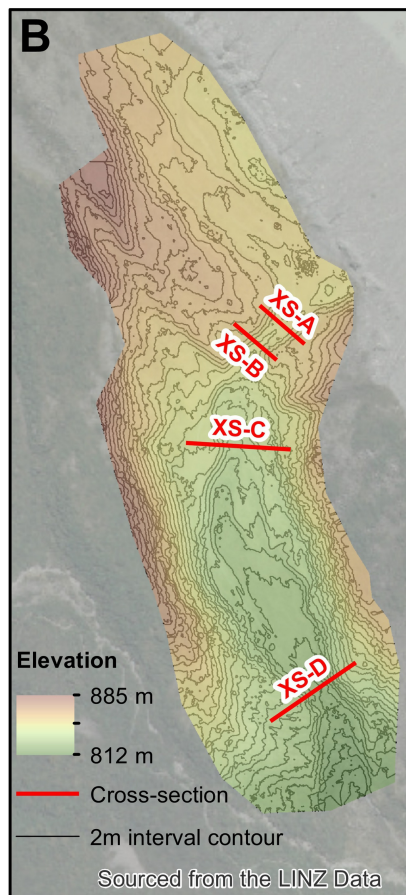


Figure 3

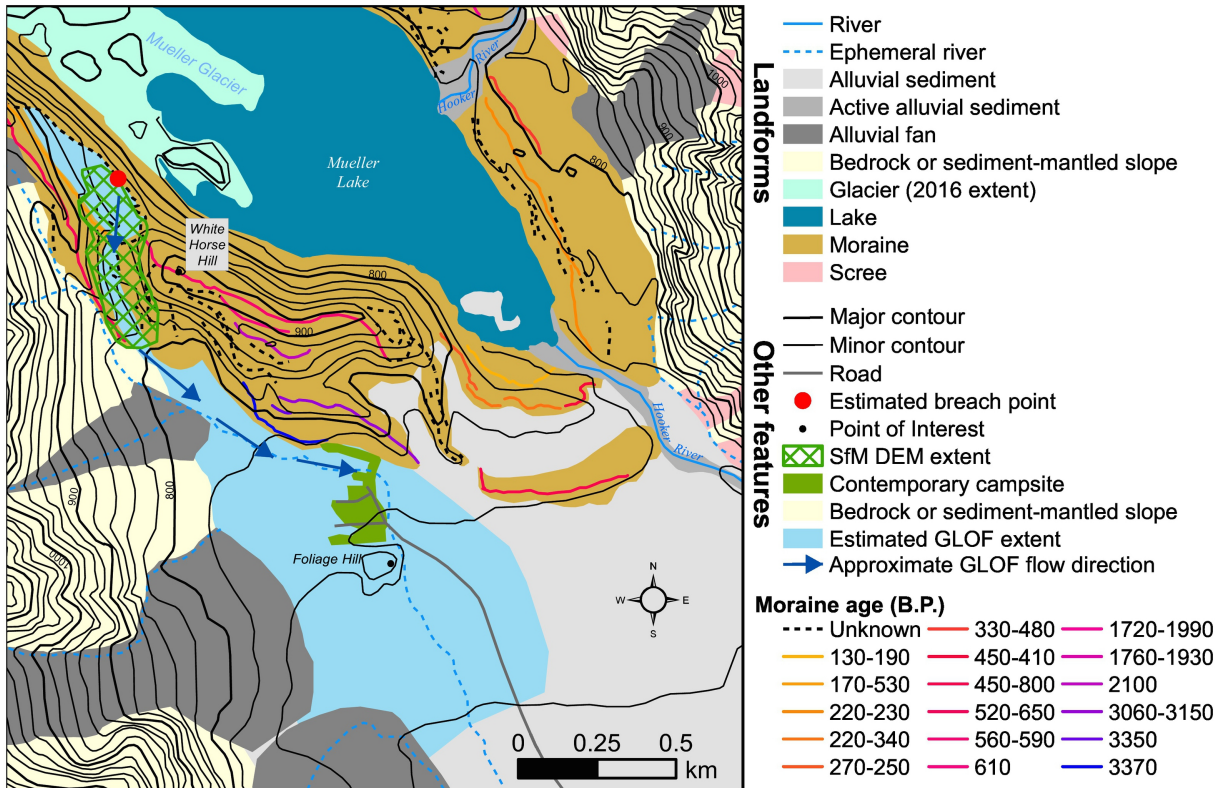


Figure 4

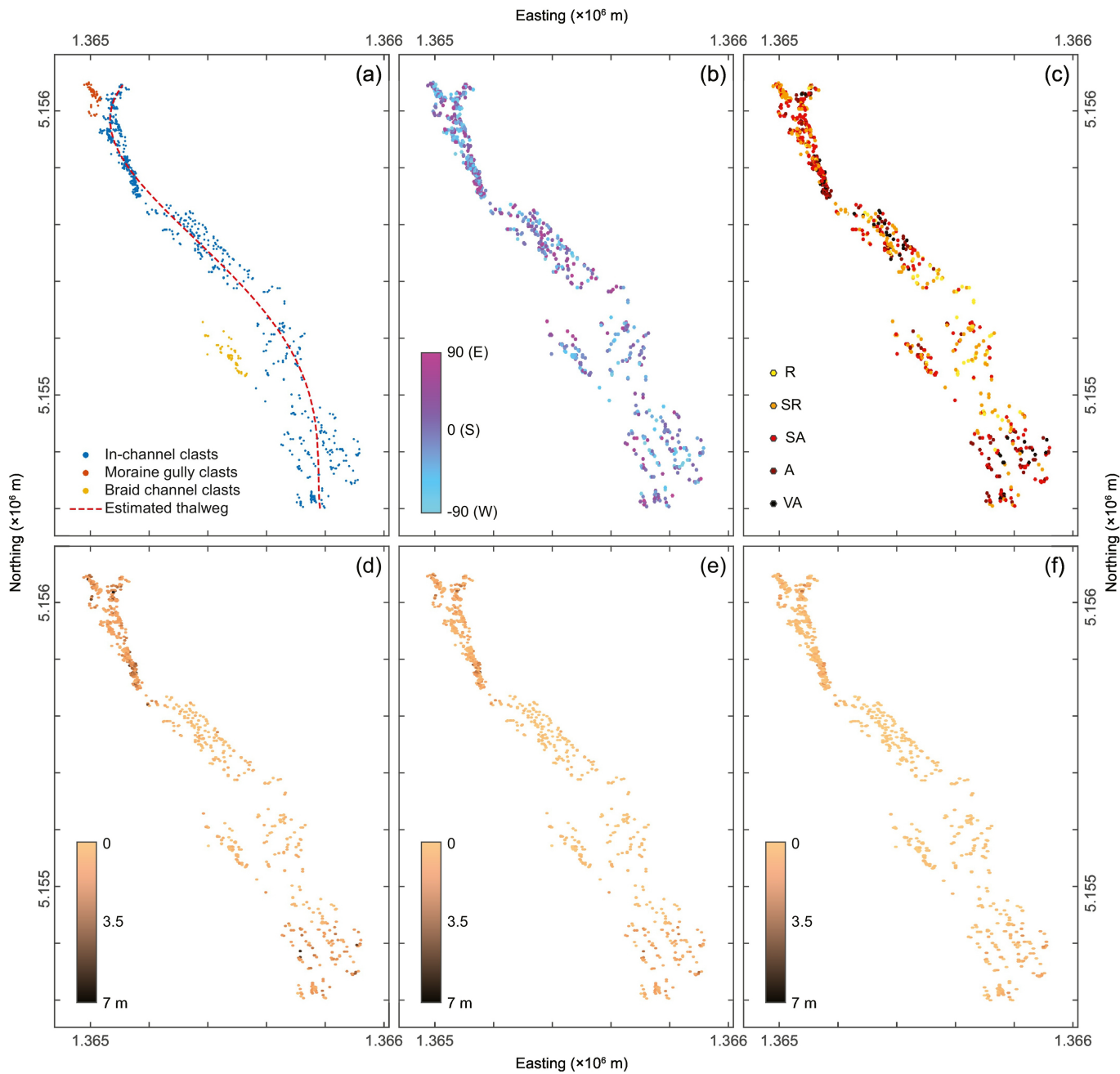


Figure 5

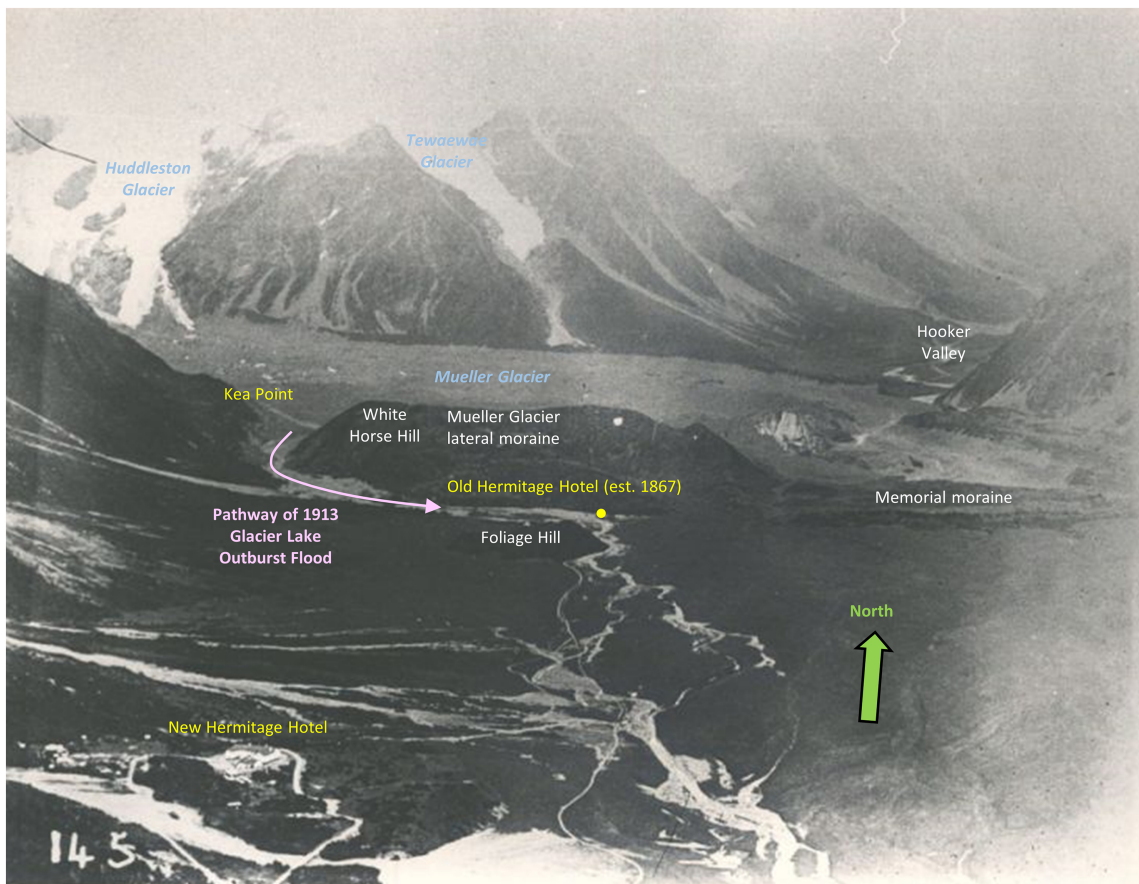


Figure 6

January 1913 flood

Legend: Date Event Resource

Triggers		Event		Geomorphological impacts	Impacts on property & people
5-21 January	18-20 January	19 January	20 January		
<ul style="list-style-type: none"> Heavy rain Snow melt 	<ul style="list-style-type: none"> Extremely heavy rainfall Flooding 	<ul style="list-style-type: none"> Lateral moraine at Kea Point breaks & flooding begins. First peak outflow @ ~ 4 pm. 	<ul style="list-style-type: none"> Second peak outflow early morning. Flood water and boulders from Mueller moraine. Increased lake water levels. Moraine breached via historic breach near Hooker River outlet. 	<ul style="list-style-type: none"> Transport of large volumes of boulders from moraine. Very large boulders, but range of sediment sizes. Also transport of vegetation & ice blocks. Erosion of new river channels. 	<ul style="list-style-type: none"> Total erosion of a road & emplacement of large boulders & debris Damage to approaches to bridges Road bridges undamaged, except foot bridges
<ul style="list-style-type: none"> Newspapers Book 	<ul style="list-style-type: none"> Newspapers Book 	<ul style="list-style-type: none"> Newspapers Letters Book 	<ul style="list-style-type: none"> Newspapers Letters Book Reports Geomorphological mapping 	<ul style="list-style-type: none"> Newspapers Book Reports Geomorphological mapping Sediment data 	<ul style="list-style-type: none"> Letters Reports Newspapers

March 1913 flood

Triggers	Event	Geomorphological impacts	Impacts on property & people
28 March	28 March		
<ul style="list-style-type: none"> Heavy rain: 9.8 inches in 23 hours at highest intensity. Wet weather for 3 months Melting of snow 	<ul style="list-style-type: none"> Flood from lateral moraine breach Flood waters carrying glacial ice. Also reports of terminal breach. Collapse of ice bridges and enlargement of drainage channels. Max estimated discharge of 1007 m³s⁻¹ 	<ul style="list-style-type: none"> Evidence suggests larger flood than Jan 1913. Falling ice blocks from Mueller's terminus. Transport of very large pieces of ice & boulders Boulders & ice blocks deposited near the Hermitage. Numerous new channels around the Hermitage. Doubling in width of Hooker River channel. 	<ul style="list-style-type: none"> Bridge over Hooker destroyed. Supports of Hermitage suspension bridge & Bushy Creek bridge damaged. Roads & bridge approaches destroyed. Wash house washed away. Front of Hermitage Hotel collapsed into stream. Damage to glacier tracks.
<ul style="list-style-type: none"> Newspapers Weather report Reports Newspapers 	<ul style="list-style-type: none"> Newspapers Reports Geomorphology Glacier reconstruction Flow modelling 	<ul style="list-style-type: none"> Newspapers Book Reports Geomorphological mapping Sediment data 	<ul style="list-style-type: none"> Reports Newspapers

Figure 7

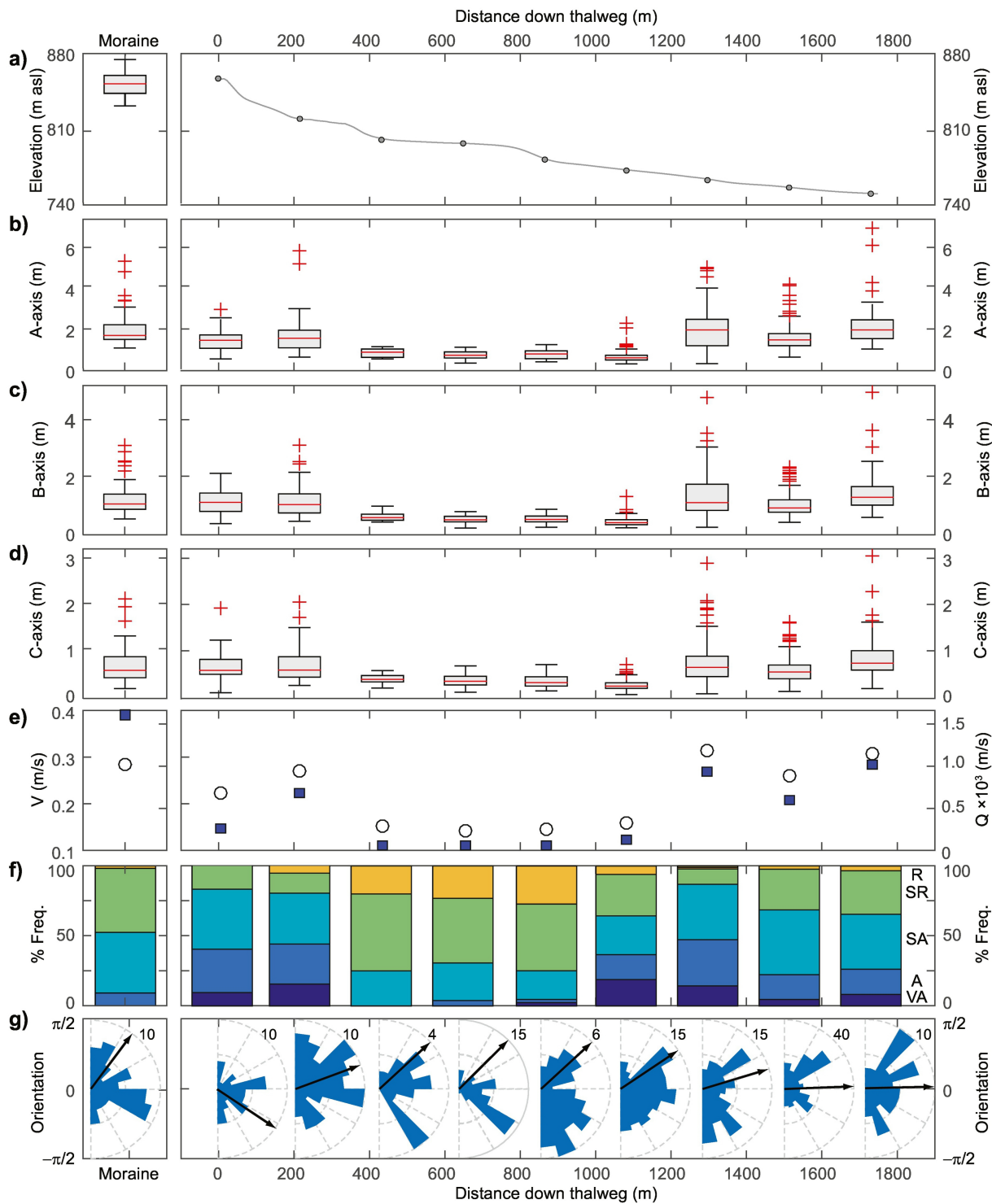


Figure 8

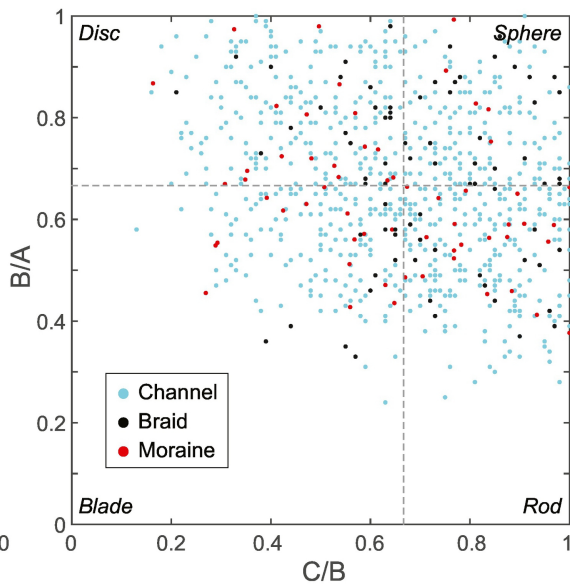
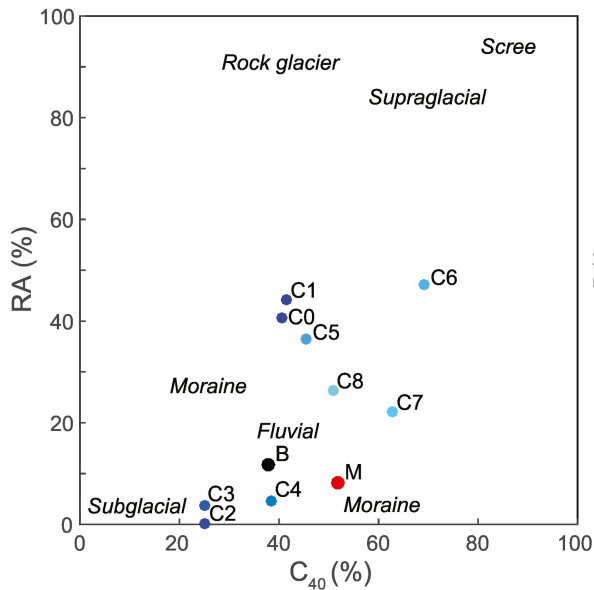


Figure 9